Accepted Manuscript

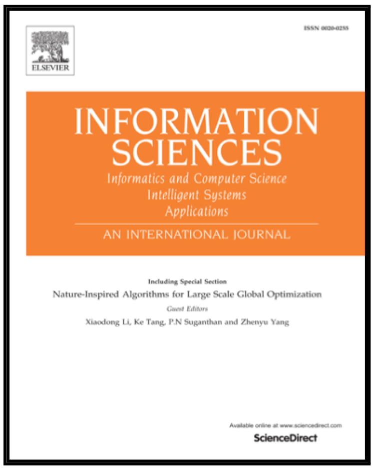

Backstepping Nussbaum Gain Dynamic Surface Control for a Class of Input and State Constrained Systems with Actuator Faults

Hamed Habibi , Hamed Rahimi Nohooji , Ian Howard

PII: S0020-0255(18)31041-7
DOI: https://doi.org/10.1016/j.ins.2018.12.084
Reference: INS 14184

To appear in: *Information Sciences*

Received date: 10 September 2018
Revised date: 30 December 2018
Accepted date: 31 December 2018

Please cite this article as: Hamed Habibi , Hamed Rahimi Nohooji , Ian Howard , Backstepping Nussbaum Gain Dynamic Surface Control for a Class of Input and State Constrained Systems with Actuator Faults, *Information Sciences* (2019), doi: https://doi.org/10.1016/j.ins.2018.12.084

Backstepping Nussbaum Gain Dynamic Surface Control for a Class of Input and State Constrained Systems with Actuator Faults

Hamed Habibi[1], Hamed Rahimi Nohooji[1,2], and Ian Howard[1]
[1]Faculty of Science and Engineering, School of Civil and Mechanical Engineering, Curtin University, Perth, WA 6845, Australia
[2]Center for Research in Mechatronics, Institute of Mechanics, Materials and Civil Engineering, Université catholique de Louvain, 1348 Louvain-la-Neuve, Belgium

Abstract
This paper presents a novel constructive control design applicable for uncertain dynamic systems subject to input and state saturations, unknown direction, and actuation faults. The controller is based on the direct Lyapunov method, which by use of the Nussbaum-type function, provides an adaptive control scheme that can handle the effect of unknown control direction. The violation of constraints is avoided by relying on the bounding of the Lyapunov function in the closed-loop system using the barrier Lyapunov function (BLF). The time-varying cotangent-type BLF is constructed, and by introducing a novel flexible technique to generate state constraints, general constraints are formed systematically to relax different initial conditions. Proper input saturation is utilized, and it is shown that under the proposed control all the signals in the closed-loop system are bounded without violating the constraints, in both fault-free and faulty actuation. The performance of the theoretical results is illustrated using numerical simulations. Also, a comparison is made with the results of well-known logarithm BLF and traditional quadratic Lyapunov functions to further evaluate the effectiveness of the proposed controller.

Keyword: Barrier Lyapunov function; Dynamic surface control; Fault tolerant control; Full state constraints; Input saturation; Nussbaum gain control; Unknown control direction.

“Declarations of interest: none”

1. Introduction.

The desired trajectory-tracking problem for nonlinear systems has drawn significant attention from both academia and industry over the last decades. This problem becomes even more challenging if uncertain system dynamics and state constraints are involved. Based on the Lyapunov stability theory, different techniques have been proposed to tackle this problem in the last few decades, e.g., adaptive position/force control [20], adaptive vision and force tracking control [3], computed torque control [31], coordinated control [19], admittance control [40], and impedance control [17]. Different from the conventional Lyapunov functions, Barrier Lyapunov Functions (BLF) grow to infinity whenever its arguments approach their bounds [39]. Accordingly, this method can be used to prevent violation of constraints along the system trajectories [34]. There exist different forms of BLF, e.g., logarithmic [30], integral [37], hyperbolic [41], tangent [33], secant [26], and cotangent [4]. This method is widely used to control dynamic systems with position [33], velocity [26] and full state [23] constraints. Accordingly, BLFs-based constrained control has been utilized in several practical systems like robotics [32] direct current (DC) motors [25], wind turbines [8], flexible structure systems [41], and aerial vehicles [1].

The unknown control direction is a major problem regarding systems with unknown parameters [23], or with time variable dynamic structures through operation [35]. This issue is considered as either indefinite control sign [23] or unknown control gain [44]. In these cases, most of the aforementioned controllers fail to operate satisfactorily in practice, because the control direction has been utilized in the controller structure [6]. The adaptive control design based on Nussbaum type functions is a suitable approach to cope with the aforementioned issues [23, 27, 36]. In this regard, the Nussbaum type function is used to modify the virtual control in the backstepping framework to relax the known control direction condition, which is a relatively strict condition, especially for unknown disturbed nonlinear systems [23].

One major drawback of the traditional backstepping design is the need for the repetitive time derivative of virtual control. This can cause drastic system proliferation, singularity and consequently undesirable system performance or even instability [29]. Also, even when the designed controller performs satisfactorily, the increased final system order is inevitable [44]. Obviously the more computationally complex the control schemes reduces the practical acceptability. This issue is more challenging if the virtual control is augmented with Nussbaum type functions. The dynamic surface control (DSC) technique was proposed to eliminate this issue [43]. In this technique at each step of the recursive backstepping approach, a first order filter is introduced to the synthetic input [6, 29, 44]. Accordingly, this method was investigated in designing control for different nonlinear systems [44] and practical systems [29]. However, very few research works have utilized this method in the design of control for nonlinear systems with unknown control direction [43, 44].

Long-term operation of the system in harsh situations may cause actuation faults which lead to degradation of system performance, system failure and instability. In the last few decades, fault tolerant control has been proposed as an appropriate scheme to remove fault effects [18]. Different reconfigurable controller designs have been proposed to accommodate the actuator faults, which are based on fault detection, isolation, and control reconfiguration to eliminate fault effects [2]. In these methods, the whole system dynamics must be known as a priori. However, in the presence of system uncertainty, disturbances and undetectable time variable faults, the mentioned methods fail to compensate for the fault effect satisfactorily [21]. Therefore, it is beneficial to design controllers to be robust against actuation faults, eliminating the requirement for fault detection and controller reconfiguration. On the other hand, the actuator effort, requested from the controller, is bounded in realistic dynamic systems. In fact, the industrial actuators are not obviously able to make a very large effort, in which case the actuator output is saturated, and fixed after the upper or lower bounds of the actuator operational range. Therefore, to have a practical scheme, it is necessary to consider the actuator input saturation in the controller design procedure. However, only in a few recent papers has the input saturation been considered in the controller design for nonlinear uncertain and disturbed dynamic systems [6, 44].

Motivated by the aforementioned considerations, this paper proposes the novel control design for a nonlinear disturbed uncertain dynamic system with unknown actuator faults and unknown control direction subject to input saturation. Cotangent-type BLF is developed via a backstepping scheme to constrain all states within asymmetric time-varying bounds. The proposed controller addresses the accrued tracking problem and ensures uniform boundedness of the system while all signals in the closed-loop system remain bounded.

The main advantages of the proposed control are as follows.
1) With respect to a recent controller designed for full state constrained control of nonlinear uncertain dynamic systems, [6, 30, 38], the proposed controller does not require control direction. In addition, compared with the recent works that can tackle the problem of unknown control direction, e.g. in [23], the repetitive virtual control differentiation in the backstepping scheme is avoided by adoption of the DSC technique.
2) A new form of BLF is proposed in this paper which can be viewed as an alternative in constrained control of dynamical systems. Also, by introducing Lemma 2 the constrained control design procedure in this paper requires fewer design parameters compared to previous works like [14-16]. In addition, with respect to the symmetric or static BLF utilized in the constrained control of dynamical systems [22, 23, 34], the proposed BLF can handle both time-varying and asymmetric constraints. Furthermore, a new scheme is proposed to generate state constraints according to initial conditions, desired trajectory and the required distance between constraints and their desired trajectories, which can relax any initial conditions on the starting values of the movement.
3) The actuator fault is modelled as effectiveness loss and bias, as well, to cover a wide variety of types of actuator faults. In addition, to avoid performance degradation as a result of significantly increasing the control signal magnitude, input saturation utilization is considered which can improve the system reliability. Note that to have all functions being differentiable in the backstepping scheme, unlike previous works like [7, 42] we employed smooth functions to bind the input.

The rest of paper is organized as follows. In Section 2, the model of the nonlinear uncertain dynamic system including input saturation and disturbance is described and some preliminaries are given. In Section 3 the controller is developed in a systematic manner and also, boundedness of the closed-loop system is proved. In Section 4 the numerical example is studied, and the designed controller performance is evaluated in both fault free and actuation fault cases. Also, a comparison is made with the results of well-known logarithm BLF and traditional quadratic Lyapunov function to further evaluate the effectiveness of the proposed controller. Finally, the conclusions are given in Section 5.

2. Problem formulation and preliminaries.

Consider the nonlinear strict feedback uncertain dynamic system as,

$$\begin{cases} \dot{x}_i = \vartheta_i^T \phi_i(\bar{x}_i) + \varphi_i x_{i+1} + d_i(\bar{x}_n, t) \\ \dot{x}_n = \vartheta_n^T \phi_n(\bar{x}_n) + \varphi_n H(u_a) + d_n(\bar{x}_n, t), \\ y = x_1 \end{cases} \tag{1}$$

where, $x \in \mathbb{R}^n$ is the system state vector, $y \in \mathbb{R}$ is the output, $u_a \in \mathbb{R}$ is the control input, $\bar{x}_i = [x_1, \dots, x_i]^T$; $\phi_i(\bar{x}_i) \in \mathbb{R}^m$ is the known nonlinear function vector, $\vartheta_i \in \mathbb{R}^m$ is the unknown constant vector, $\varphi_i \in \mathbb{R}$ is the unknown constant number and $d_i(\bar{x}_n, t) \in \mathbb{R}$ is the unknown bounded external disturbance for $i = 1, \dots, n$.
Remark 1: Many practical systems can be represented as (1), e.g. crane system [11], robotic manipulator [12] and offshore wind turbine [10].

The function $H(u_a)$ is an asymmetric non-smooth input saturation with unknown time varying slope, as,

$$H(u_a) = \begin{cases} \bar{\varrho}, & u_a > \bar{u}_a \\ l u_a, & -\underline{u}_a \le u_a \le \bar{u}_a \\ -\underline{\varrho}, & u_a < -\underline{u}_a, \end{cases} \tag{2}$$

where, $\bar{\varrho}$ and $\underline{\varrho}$ are known constant bounds of the input, $\bar{u}_a$ and $\underline{u}_a$ represents positive input break points and l is an unknown time varying function which represents input slope. $H(u_a)$ is illustrated schematically in Figure 1.

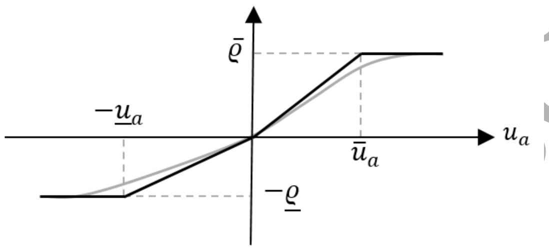

Fig. 1. Schematics of input saturation $H(u_a)$ (black line) and its smooth estimation $S(u_a)$ (grey line).

A smooth function $S(u_a)$ is defined to cope with the asymmetric non-smooth input saturation as,

$$S(u_a) = \frac{\bar{\varrho}\mathrm{P} - \underline{\varrho}\mathrm{P}^{-1}}{\mathrm{P} + \mathrm{P}^{-1}}, \tag{3}$$

where, $\mathrm{P} = e^{\epsilon + \eta u_a}$, $\epsilon = 0.5\ln(\underline{\varrho}/\bar{\varrho})$ and η is a positive constant. $S(u_a)$ always stays in the range $(-\underline{\varrho}, \bar{\varrho})$ for all $u_a \in \mathbb{R}$, as illustrated schematically in Figure 1.

Remark 2: Two other common types of input saturation can be considered, including asymmetric non-smooth saturation with unknown constant slope, and asymmetric non-smooth saturation with dead zone [44]. For the unknown constant slope case, l is a constant number in (2), and for the dead zone case $H(u_a) = 0$ for $-\underline{m}_a \le u_a \le \bar{m}_a$, where, $\underline{m}_a$ and $\bar{m}_a$ represent the break points. Input saturation model (2) can be simply modified to include these issues. However, without loss of generality, asymmetric non-smooth input saturation with unknown time varying slope is only considered in this paper.

Now, $H(u_a)$ is estimated as,

$$H(u_a) = S(u_a) + D(u_a), \tag{4}$$

where, $D(u_a)$ is the estimation error of $H(u_a)$. Considering the bounded property of $H(u_a)$ and $S(u_a)$, $D(u_a)$ is bounded as $|D(u_a)| \le \bar{D}$, where $\bar{D}$ is an unknown positive constant. As $S(u_a)$ is a nonaffine function of u_a, the mean value theorem is employed to have $S(u_a)$ represented as an affine function of u_a, as,

$$S(u_a) = S(u_{a0}) + \left.\frac{\partial S}{\partial u_a}\right|_{u_{ak}} (u_a - u_{a0}), \tag{5}$$

where, $u_{ak} = \Xi u_a + (1 - \Xi) u_{a0}$ with $\Xi \in (0,1)$. Considering $S(0) = 0$, then $u_{a0} = 0$ is an appropriate choice. Accordingly, (5) becomes,

$$S(u_a) = g_s u_a, \tag{6}$$

where, $g_s = \partial S / \partial u_a|_{\Xi u_a} = 2\eta(\underline{\varrho} + \bar{\varrho})/(\mathrm{P} + \mathrm{P}^{-1})^2$. For any $u_a \in \mathbb{R}$, g_s is positive and bounded as $g_s \le \bar{g}_s$, where $\bar{g}_s$ is a positive constant.

It should be noted that when the actuator deviates from normal operation, the control input u_a will not be identical to the designed control input u_d, anymore. This faulty actuation is modelled as,

$$u_a = \rho_f(t_\rho, t)u_d + \phi_f(t_\phi, t), \tag{7}$$

where, $u_d \in \mathbb{R}$ is the designed control input, $\rho_f(t_\rho, t)$ implies the time variable unknown effectiveness loss of the actuator that happens at unknown time t_ρ and $\phi_f(t_\phi, t)$ is the unknown time variable additive actuator fault, i.e. actuator bias, that occurs at unknown time t_ϕ.

Thus, considering (4), (6) and (7), the nonlinear system (1) can be rewritten as,

$$\begin{cases} \dot{x}_i = \vartheta_i^T \phi_i(\bar{x}_i) + \varphi_i x_{i+1} + d_i(\bar{x}_n, t) \\ \dot{x}_n = \vartheta_n^T \phi_n(\bar{x}_n) + \varphi_n g_s(\rho_f u_d + \phi_f) + \varphi_n D + d_n(\bar{x}_n, t) \\ y = x_1. \end{cases} \tag{8}$$

The main control objective of this paper is to design a state feedback adaptive control such that, *(i)* to guarantee that the output y tracks the known bounded desired reference signal $x_d(t)$ in a bounded compact set $\Omega_y := \{y(t) \in \mathbb{R}: \underline{k}_{c_1}(t) < y(t) < \bar{k}_{c_1}(t)\}$ where $\underline{k}_{c_1}(t)$ and $\bar{k}_{c_1}(t)$ are bounded predefined functions, *(ii)* to constrain all system states in the compact set, $\Omega_{x_i} := \{x_i(t) \in \mathbb{R}: \underline{k}_{c_i}(t) < x_i(t) < \bar{k}_{c_i}(t)\}$ for $i = 2, \ldots, n$, where $\underline{k}_{c_i}(t)$ and $\bar{k}_{c_i}(t)$ are bounded predefined functions, *(iii)* all signals in the closed-loop system are bounded, despite the presence of actuator faults, unknown external disturbances and input saturation.

To initiate the control design, the following assumptions are made in the design procedure.

Assumption 1: Effectiveness loss of the actuator is assumed to be bounded as $0 < \underline{\lambda} \le \rho_f \le 1$. In fact, $\rho_f = 1$ indicates full effectiveness of the actuator. Also, $\underline{\lambda}$ is a positive number which means that the actuator will not totally fail to operate. However, if the actuation redundancy is already available in the system structure, the developed method in this paper can also be applicable for $\rho_f = 0$. On the other hand, considering bounded achievable actuator effort, actuator bias is assumed to be bounded as, $|\phi_f| \le \bar{\phi} < \infty$, where $\bar{\phi}$ is an unknown positive number.

Assumption 2: The constant φ_i with $i = 1, \ldots, n$, in (1), and (8) are unknown and also, $\varphi_i \ne 0$ to satisfy the controllability condition. Also, $|\varphi_i| < k_{\varphi_i}$, where k_{φ_i} is a known positive number.

Assumption 3: There exist functions $\underline{K}_{c_0}(t)$ and $\bar{K}_{c_0}(t)$, satisfying $\underline{k}_{c_1}(t) \le \underline{K}_{c_0}(t)$ and $\bar{K}_{c_0}(t) \le \bar{k}_{c_1}(t)$, such that $\underline{K}_{c_0}(t) < x_d(t) < \bar{K}_{c_0}(t)$. Also, there exist positive constants $\bar{K}_{c_i}$ and $\underline{K}_{c_i}$, such that, $\left|\dot{\bar{k}}_{c_i}(t)\right| \le \bar{K}_{c_i}$ and $\left|\dot{\underline{k}}_{c_i}(t)\right| \ge \underline{K}_{c_i}$. Also, the j^{th} derivative of the desired trajectory, $x_d^{(j)}(t)$ for $j = 1, \ldots, n-1$ are assumed to satisfy $\left|x_d^{(j)}(t)\right| \le A_j$, where A_j are positive constants. Accordingly, a compact set Ω_{x_d} is defined as $\Omega_{x_d} := \{x_d \in \mathbb{R}: x_d^2 + \dot{x}_d^2 + \ddot{x}_d^2 < \delta_{x_d}\}$, which will be used in the control design.

Assumption 4: There exist positive constants $\bar{k}_{u_i}$, $\underline{k}_{u_i}$, $\bar{k}_{l_i}$ and $\underline{k}_{l_i}$, such that $\underline{k}_{u_i} < k_{u_i}(t) < \bar{k}_{u_i}$ and $\underline{k}_{l_i} < k_{l_i}(t) < \bar{k}_{l_i}$ for $i = 1, \ldots, n$, where $k_{u_i}(t)$ and $k_{l_i}(t)$ are time varying barriers on the error, defined as, $k_{u_i}(t) = \bar{k}_{c_i}(t) - x_d^{(i-1)}(t)$ and $k_{l_i}(t) = \underline{k}_{c_i}(t) - x_d^{(i-1)}(t)$. The aforementioned bounds for an example of the desired trajectory are demonstrated in Figure 2, in which the bounds are depicted exaggeratedly far from each other for the sake of illustration.

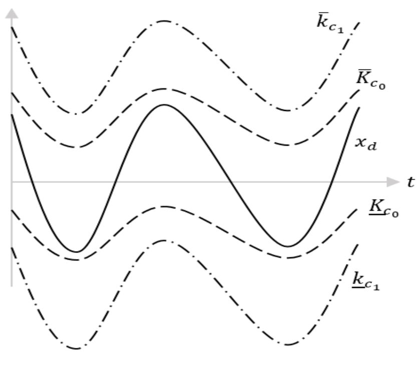

Fig. 2. An example of the desired trajectory, x_d, along with lower bounds $\underline{k}_{c_1}$ and $\underline{K}_{c_0}$, and upper bounds $\bar{k}_{c_1}$ and $\bar{K}_{c_0}$.

Assumption 5: External disturbances $d_i(\bar{x}_n, t)$ with $i = 1, \dots, n$ are assumed to be unknown but bounded as, $|d_i| \le \bar{d}_i$, where $\bar{d}_i$ is an unknown positive constant.

Remark 3. Some lower and upper bounds are defined in Assumptions 1, 3, and 4 in formulating the control problem. These bounds are used to analyse the stability of the closed-loop system augmented with the developed controller. Nevertheless, these parameters will not be used in the designed control structure. So, the actual estimation will not be required in setting up and implementing the control scheme.

Remark 4: Assumption 1 is made to ensure that there is always an actuator effort. Even though not full effort, the actuator will still have an output. On the other hand, the actuator bias cannot infinitely increase. In fact, Assumption 1 is a practical issue which implies that the actuator effort, even if not accurate, is bounded. In Assumption 2, the known boundedness of φ_i can be found in many nonlinear real systems, e.g. wind turbines [10]. In Assumption 3, the desired trajectory is assumed to be smooth and bounded. In fact, it is assumed that the desired trajectory will not change infinitely and abruptly, which is the case for most practical engineering dynamic systems. Accordingly, some useful bounds are defined in Assumption 4. Finally, in Assumption 5, the external disturbance is assumed to be bounded, which stems from the physical nature of any source which applies an external disturbance on the system.

The Nussbaum type function is introduced here, which is utilized to eliminate the unknown control direction φ_i, as per the following definition.

Definition 1 [36, 44]: Any smooth continuous even function $N(\zeta(t))$ is called a Nussbaum type function, if it satisfies the following properties.

$$\begin{aligned} &\lim_{r\to\infty} \sup \frac{1}{r}\int_0^r N(\zeta) d\,\zeta = +\infty, \\ &\lim_{r\to\infty} \inf \frac{1}{r}\int_0^r N(\zeta) d\,\zeta = -\infty. \end{aligned} \tag{9}$$

The BLF function is defined as follows, which is used in the constraint control construction.

Definition 2 [34]: A scalar function $V(x)$ is a BLF if it is a positive definite continuous scalar function, defined with respect to the system $\dot{x} = f(x)$ on an open region $\mathcal{D}$, containing the origin. In addition, $V(x)$ has continuous first order partial derivatives within all $\mathcal{D}$, and approaches to infinity as x approaches to the boundary of the region $\mathcal{D}$. Finally, $V(x)$ satisfies $V(x) \le \mathcal{w}$, $\forall t \ge 0$ along the solution of $\dot{x} = f(x)$ for $x(0) \in \mathcal{D}$, and some positive constant $\mathcal{w}$.

In this paper $V(x) = cot(\pi(1 - (x/k_e)^2)/2)$ is introduced as the BLF, which is positive definite continuous within $(-k_e, k_e)$, where k_e is a known variable which represents the boundary. On the other hand, $V(x) \to \infty$ as x approaches to $\pm k_e$.

The following definition will be used to study the stability of the closed-loop system associated with the proposed controller.

Definition 3 [28]: The solution of a system $x(t)$ is Uniformly Ultimately Bounded (UUB) if, there exists a number $T(K, x(t_0))$, and a $K > 0$ such that for any compact set $\mathcal{S}$ and all $x(t_0) \in \mathcal{S}$, $\|x(t)\| \le K$, for all $t \ge t_0 + T$.

The following lemmas are needed to be used in the closed-loop system stability analysis.

Lemma 1 [36, 44]: Assume $V(t) > 0$ and $\zeta(t)$ are smooth functions defined on the time interval $[0\ t_f)$. Also, $N(\zeta(t))$ is a selected Nussbaum type function. Then, for any $t \in [0\ t_f)$, if $V(t) < c_0 + e^{-c_1 t}\int_0^t \big(g(\tau)N(\zeta(\tau)) + 1\big)\dot{\zeta} e^{c_1\tau} d\tau$ holds true, where c_0 and c_1 are positive constants, and $g(\tau)$ is a time-varying parameter, which takes values in the unknown closed intervals $L \in [\mathrm{l}^+, \mathrm{l}^-]$ with $0 \notin L$, then $V(t)$, $\zeta(t)$ and $\int_0^t g(\tau)N(\zeta(\tau))\,\dot{\zeta} e^{c_1\tau} d\tau$ must be bounded on $[0\ t_f)$.

Lemma 2: For any variable $\psi(t)$ in $|\psi| < 1$, $\cot(\pi(1 - \psi^2)/2) \le \pi\psi^2 csc^2(\pi(1 - \psi^2)/2)$ holds true.

Proof. Define $\Delta_1 = \pi\psi^2 csc^2(\pi(1 - \psi^2)/2) - \cot(\pi(1 - \psi^2)/2)$ and $\Delta_2 = \pi\psi^2 - \sin(\pi(1 - \psi^2)/2)\cos(\pi(1 - \psi^2)/2)$. Thus, $\partial\Delta_2/\partial\psi = \pi\psi(2 - \cos(\pi(1 - \psi^2)))$. Obviously, $\partial\Delta_2/\partial\psi < 0$ for $\psi < 0$, $\partial\Delta_2/\partial\psi = 0$ for $\psi = 0$ and $\partial\Delta_2/\partial\psi > 0$ for $\psi > 0$. Accordingly, considering $\Delta_2(0) = 0$, it can be obtained that $\Delta_2 \ge 0$. Also, considering $\Delta_2 = \Delta_1 csc^2(\pi(1 - \psi^2)/2)$ and $csc^2(\bullet) > 0$, yield $\Delta_1 \ge 0$. This completes the proof. ■

It is worth noting that with the aim of Lemma 2, less parameters are required in the stability analysis of the closed-loop system associated with the proposed controller, compared to constrained controllers presented at [14-16].

Lemma 3: $0 \le |\xi| - \xi^2/\sqrt{\xi^2+\gamma^2} < \gamma$ holds true, for any variable ξ and positive constant γ.

Proof. Consider the inequality $\xi^4 \le \xi^2\gamma^2 + \xi^4$ and take the square root from both sides. Consequently, it proves the left side of the inequality. To prove the right side, consider $0 \le 2|\xi|\gamma$ and add $\xi^2+\gamma^2$ to both sides. Taking the square root of the resulted inequality leads to $\sqrt{\xi^2+\gamma^2} \le \gamma + |\xi|$. Accordingly, it can be obtained that $-1/\sqrt{\xi^2+\gamma^2} \le -1/(\gamma+|\xi|)$ which leads to $|\xi| - \xi^2/\sqrt{\xi^2+\gamma^2} \le |\xi| - \xi^2/(\gamma+|\xi|)$. Finally, considering $|\xi| - \xi^2/(\gamma+|\xi|) = \gamma|\xi|/(\gamma+|\xi|)$ and $\gamma|\xi|/(\gamma+|\xi|) < \gamma$, it can be seen that $|\xi| - \xi^2/\sqrt{\xi^2+\gamma^2} < \gamma$. This completes the proof. ■

3. Full state constrained fault tolerant control design with unknown control gain.

In this section, an adaptive full state constrained fault tolerant control is developed for the dynamic system given by (1) with input saturation (2) and actuation fault (7) in the backstepping framework to satisfy control objectives given in Section II. Also, systematic generation of the state constraints is stated. Finally, the controller design algorithm is given.

3.1. Controller design and stability analysis.

Step 1: Define error signals $e_1 = x_1 - x_d$, and $e_2 = x_2 - z_2$, where z_2 is a virtual control. Introduce a filtering of z_2 via α_1 which is a stabilizing function to be designed. Let α_1 pass through a first order filter with a time constant τ_2 as,

$$\tau_2\dot{z}_2 + z_2 = \alpha_1, z_2(0) = \alpha_1(0). \tag{10}$$

Define the output error of the first-order filter as, $\chi_2 = z_2 - \alpha_1$ where its first-time derivative yields $\dot{z}_2 = -\chi_2/\tau_2$.

Choose a positive definite Lyapunov function as,

$$V_1 = \frac{k_{e_1}^2}{\pi} cot\Lambda_1 + \frac{1}{2}\tilde{\vartheta}_1^T\Gamma_1^{-1}\tilde{\vartheta}_1 + \frac{1}{2}\chi_2^2 + \frac{1}{2}\tilde{d}_1^2, \tag{11}$$

where, the bounding $k_{e_1} = k_{u_1}$, if $e_1 > 0$, otherwise $k_{e_1} = k_{l_1}$, $\Lambda_1 = \pi(1-\xi_1^2)/2$ with $\xi_1 = \varpi(e_1)e_1/k_{u_1} + (1-\varpi(e_1))e_1/k_{l_1}$, with $\varpi(e_1) = 1$ if $e_1 > 0$, otherwise $\varpi(e_1) = 0$; $\Gamma_1 = \Gamma_1^T > 0$ is design matrix, $\tilde{\vartheta}_1 = \hat{\vartheta}_1 - \vartheta_1$ and $\tilde{d}_1 = \hat{d}_1 - \bar{d}_1$, where $\hat{\vartheta}_1$ and $\hat{d}_1$ are estimations of ϑ_1 and $\bar{d}_1$, respectively. The Lyapunov function V_1 is positive definite and continuously differentiable, also C^1 in the set $\Omega_{e_1} = \{e_1 : k_{l_1} < e_1 < k_{u_1}\}$, in which the first term captures the BLF characteristics, as explained in Definition 2, of the modified tracking error ξ_1. The first-time derivative of (11), can be obtained as,

$$\dot{V}_1 = \frac{2k_{e_1}\dot{k}_{e_1}}{\pi} cot\Lambda_1 + k_{e_1}^2\xi_1\dot{\xi}_1 csc^2\Lambda_1 + \tilde{\vartheta}_1^T\Gamma_1^{-1}\dot{\hat{\vartheta}}_1 + \chi_2\dot{\chi}_2 + \tilde{d}_1\dot{\hat{d}}_1. \tag{12}$$

Considering the definition of ξ_1 and χ_2, with dynamic response of x_2, the time derivative of ξ_1 is obtained as,

$$\dot{\xi}_1 = \varpi(e_1)\frac{\left(\vartheta_1^T\phi_1 + \varphi_1(e_2+\chi_2+\alpha_1) + d_1 - \dot{x}_d - e_1\frac{\dot{k}_{u_1}}{k_{u_1}}\right)}{k_{u_1}} + \left(1-\varpi(e_1)\right)\frac{\left(\vartheta_1^T\phi_1 + \varphi_1(e_2+\chi_2+\alpha_1) + d_1 - \dot{x}_d - e_1\frac{\dot{k}_{l_1}}{k_{l_1}}\right)}{k_{l_1}}. \tag{13}$$

Design virtual control α_1 as,

$$\alpha_1 = N(\zeta_1)\omega_1, \tag{14}$$

with,

$$\omega_1 = \hat{\vartheta}_1^T\phi_1 - \dot{x}_d + \gamma_1 e_1 + \frac{1}{2}e_1 csc^2\Lambda_1 - e_1\frac{\dot{k}_{e_1}}{k_{e_1}} + \frac{\sin(2\Lambda_1)k_{e_1}\dot{k}_{e_1}}{\pi e_1} + \hat{d}_1\frac{e_1 csc^2\Lambda_1}{\sqrt{e_1^2 csc^4\Lambda_1 + \gamma_{d_1}^2}}, \tag{15}$$

and

$$\dot{\zeta}_1 = e_1\omega_1 csc^2\Lambda_1, \tag{16}$$

where, γ_1 and γ_{d_1} are positive design parameters. Also construct the adaption laws $\hat{\vartheta}_1$ and $\hat{d}_1$ as,

$$\dot{\hat{\vartheta}}_1 = \Gamma_1(e_1\phi_1 csc^2\Lambda_1 - \mu_1\hat{\vartheta}_1), \tag{17}$$

$$\dot{\hat{d}}_1 = \frac{e_1^2 csc^4\Lambda_1}{\sqrt{e_1^2 csc^4\Lambda_1 + \gamma_{d_1}^2}} - \mu_{d_1}\hat{d}_1, \tag{18}$$

where, μ_1, μ_{d_1} are positive design parameters.

Now, using (14)-(18) and considering $\dot{\chi}_2 = -\chi_2/\tau_2 - \dot{\alpha}_1$, $\dot{V}_1$ presented in (12) can be rewritten as,

$$\dot{V}_1 = \varphi_1 N(\zeta_1)\dot{\zeta}_1 + \dot{\zeta}_1 - \gamma_1 e_1^2 csc^2\Lambda_1 - \frac{\chi_2^2}{\tau_2} + \varphi_1 e_1 e_2 csc^2\Lambda_1 + e_1\varphi_1\chi_2 csc^2\Lambda_1 - \mu_1\tilde{\vartheta}_1^T\hat{\vartheta}_1 - \dot{\alpha}_1\chi_2 - \frac{1}{2}e_1^2 csc^4\Lambda_1 - \mu_{d_1}\hat{d}_1\tilde{d}_1 + d_1 e_1 csc^2\Lambda_1 - \bar{d}_1\frac{e_1^2 csc^4\Lambda_1}{\sqrt{e_1^2 csc^4\Lambda_1 + \gamma_{d_1}^2}}. \tag{19}$$

Since α_1 is a function of $\bar{x}_1$, x_d, $\dot{x}_d$ and estimated variables $\hat{\vartheta}_1$ and $\hat{d}_1$, it can be shown that

$$\dot{\alpha}_1 = \frac{\partial\alpha_1}{\partial\bar{x}_1}\dot{\bar{x}}_1 + \frac{\partial\alpha_1}{\partial x_d}\dot{x}_d + \frac{\partial\alpha_1}{\partial\dot{x}_d}\ddot{x}_d + \frac{\partial\alpha_1}{\partial\hat{\vartheta}_1}\dot{\hat{\vartheta}}_1 + \frac{\partial\alpha_1}{\partial\hat{d}_1}\dot{\hat{d}}_1. \tag{20}$$

Considering (20), $\dot{\alpha}_1$ is a continuous function and has a maximum constant value M_1 in the compact set $\Omega_{x_d}\times\Omega_1$, for given initial conditions, where $\Omega_1 := \{[e_1, \tilde{\vartheta}_1, \tilde{d}_1, \chi_2]^T : (k_{e_1}^2 cot\Lambda_1)/\pi + \frac{1}{2}\tilde{\vartheta}_1^T\Gamma_1^{-1}\tilde{\vartheta}_1 + \frac{1}{2}\chi_2^2 + \frac{1}{2}\tilde{d}_1^2 < \delta_1\}$ [29, 44]. So, based on Young's inequality,

$$\begin{aligned} |\dot{\alpha}_1\chi_2| &\le \frac{\chi_2^2}{2} + \frac{M_1^2}{2}, \\ \varphi_1 e_1 e_2 csc^2\Lambda_1 &\le \frac{\varphi_1^2 e_2^2}{2} + \frac{e_1^2 csc^4\Lambda_1}{2}, \\ e_1\varphi_1\chi_2 csc^2\Lambda_1 &\le k_{\varphi_1} csc^2\Lambda_1\left(\frac{e_1^2}{2} + \frac{\chi_2^2}{2}\right). \end{aligned} \tag{21}$$

Also, it is easy to obtain,

$$\begin{aligned} -\mu_1\tilde{\vartheta}_1^T\hat{\vartheta}_1 &\le -\frac{1}{2}\mu_1\|\tilde{\vartheta}_1\|^2 + \frac{1}{2}\mu_1\|\vartheta_1\|^2, \\ -\mu_{d_1}\hat{d}_1\tilde{d}_1 &\le -\frac{1}{2}\mu_{d_1}\tilde{d}_1^2 + \frac{1}{2}\mu_{d_1}\bar{d}_1^2. \end{aligned} \tag{22}$$

Finally, according to Lemma 3,

$$d_1 e_1 csc^2\Lambda_1 - \bar{d}_1\frac{e_1^2 csc^4\Lambda_1}{\sqrt{e_1^2 csc^4\Lambda_1 + \gamma_{d_1}^2}} < \bar{d}_1\gamma_{d_1}. \tag{23}$$

According to (21)-(23) and considering Lemma 2, (19) is rewritten as,

$$\dot{V}_1 \le \varphi_1 N(\zeta_1)\dot{\zeta}_1 + \dot{\zeta}_1 - \sigma_{1,1}V_1 + \sigma_{2,1} + \frac{\varphi_1^2 e_2^2}{2}, \tag{24}$$

where, $\sigma_{1,1} = \min\{K_{1,1}, K_{2,1}, \mu_1/\lambda_{max}(\Gamma_1^{-1}), \mu_{d_1}\}$, $\sigma_{2,1} = \mu_1\|\vartheta_1\|^2/2 + M_1^2/2 + \mu_{d_1}\bar{d}_1^2/2 + \bar{d}_1\gamma_{d_1}$, $K_{1,1} = \gamma_1 - k_{\varphi_1}/2$ and $K_{2,1} = 1/\tau_2 - k_{\varphi_1}csc^2\Lambda_1/2 - 1/2$. It should be noted that $\lambda_{max}(\mathcal{A})$ represents the maximum eigenvalue of matrix $\mathcal{A}$. The selection of ranges of the design parameters γ_1 and τ_2 are as $\gamma_1 > k_{\varphi_1}/2$ and $\tau_2 < 2/(k_{\varphi_1}csc^2\Lambda_1 + 1)$, respectively, to guarantee that $K_{1,1}$ and $K_{2,1}$ are positive.

Step $i, i = 2, \dots, n-1$: Define $e_i = x_i - z_i$, where z_i is a virtual control. Introduce a filtering of z_i via α_{i-1} which is a stabilizing function to be designed. Let α_{i-1} pass through a first order filter with a time constant τ_i as,

$$\tau_i\dot{z}_i + z_i = \alpha_{i-1}, z_i(0) = \alpha_{i-1}(0). \tag{25}$$

Define the output error of the first-order filter as, $\chi_i = z_i - \alpha_{i-1}$ where its first-time derivative yields $\dot{z}_i = -\chi_i/\tau_i$. Choose a positive definite Lyapunov function as,

$$V_i = \frac{k_{e_i}^2}{\pi}cot\Lambda_i + \frac{1}{2}\tilde{\vartheta}_i^T\Gamma_i^{-1}\tilde{\vartheta}_i + \frac{1}{2}\chi_{i+1}^2 + \frac{1}{2}\tilde{d}_i^2, \tag{26}$$

where, $k_{e_i} = k_{u_i}$, if $e_i > 0$, otherwise $k_{e_i} = k_{l_i}$, $\Lambda_i = \pi(1-\xi_i^2)/2$, $\xi_i = \varpi(e_i)e_i/k_{u_i} + (1-\varpi(e_i))e_i/k_{l_i}$, with $\varpi(e_i) = 1$ if $e_i > 0$, otherwise $\varpi(e_i) = 0$, $\Gamma_i = \Gamma_i^T > 0$ is the design matrix, $\tilde{\vartheta}_i = \hat{\vartheta}_i - \vartheta_i$ and $\tilde{d}_i = \hat{d}_i - \bar{d}_i$, where $\hat{\vartheta}_i$ and $\hat{d}_i$ are estimations of ϑ_i and $\bar{d}_i$, respectively. It should be noted that V_i is continuous in the set $\Omega_{e_i} = \{e_i : k_{l_i} < e_i < k_{u_i}\}$. The Lyapunov function V_i is positive definite, in which the first term captures the BLF characteristics of the modified tracking error ξ_i. The first-time derivative of (26), can be obtained as,

$$\dot{V}_i = \frac{2k_{e_i}\dot{k}_{e_i}}{\pi} cot\Lambda_i + k_{e_i}^2 \xi_i \dot{\xi}_i csc^2\Lambda_i + \tilde{\vartheta}_i^T \Gamma_i^{-1} \dot{\hat{\vartheta}}_i + \chi_{i+1}\dot{\chi}_{i+1} + \tilde{d}_i \dot{\hat{d}}_i. \tag{27}$$

Considering the definition of ξ_i and χ_i, with dynamic response of x_{i+1}, the time derivative of ξ_i is obtained as,

$$\dot{\xi}_i = \varpi(e_i) \frac{\left(\vartheta_i^T \phi_i + \varphi_i(e_{i+1} + \chi_{i+1} + \alpha_i) + d_i + \frac{\chi_i}{\tau_i} - e_i \frac{\dot{k}_{u_i}}{k_{u_i}}\right)}{k_{u_i}} + \left(1 - \varpi(e_i)\right) \frac{\left(\vartheta_i^T \phi_i + \varphi_i(e_{i+1} + \chi_{i+1} + \alpha_i) + d_i + \frac{\chi_i}{\tau_i} - e_i \frac{\dot{k}_{l_i}}{k_{l_i}}\right)}{k_{l_i}}. \tag{28}$$

Design virtual control α_i as,

$$\alpha_i = N(\zeta_i)\omega_i, \tag{29}$$

with,

$$\omega_i = \hat{\vartheta}_i^T \phi_i + \frac{\chi_i}{\tau_i} + \gamma_i e_i + \frac{1}{2} e_i csc^2\Lambda_i - e_i \frac{\dot{k}_{e_i}}{k_{e_i}} + \frac{\sin(2\Lambda_i) k_{e_i} \dot{k}_{e_i}}{\pi e_i} + \hat{d}_i \frac{e_i csc^2 \Lambda_i}{\sqrt{e_i^2 csc^4\Lambda_i + \gamma_{d_i}^2}}, \tag{30}$$

and,

$$\dot{\zeta}_i = e_i \omega_i csc^2\Lambda_i, \tag{31}$$

where, γ_i and γ_{d_i} are positive design parameters. Also, construct the adaption laws $\hat{\vartheta}_i$ and $\hat{d}_i$ as,

$$\dot{\hat{\vartheta}}_i = \Gamma_i(e_i \phi_i csc^2\Lambda_i - \mu_i \hat{\vartheta}_i), \tag{32}$$

$$\dot{\hat{d}}_i = \frac{e_i^2 csc^4\Lambda_i}{\sqrt{e_i^2 csc^4\Lambda_i + \gamma_{d_i}^2}} - \mu_{d_i} \hat{d}_i, \tag{33}$$

where, μ_i and μ_{d_i} are positive design parameters.

Now, using (29)-(33) and considering $\dot{\chi}_{i+1} = -\chi_{i+1}/\tau_{i+1} - \dot{\alpha}_i$, $\dot{V}_i$, using (27), it can be rewritten as,

$$\begin{aligned}\dot{V}_i = \varphi_i N(\zeta_i)\dot{\zeta}_i + \dot{\zeta}_i - \gamma_i e_i^2 csc^2\Lambda_i - \frac{\chi_{i+1}^2}{\tau_{i+1}} + \varphi_i e_i e_{i+1} csc^2\Lambda_i + e_i \varphi_i \chi_{i+1} csc^2\Lambda_i - \mu_i \tilde{\vartheta}_i^T \hat{\vartheta}_i - \dot{\alpha}_i \chi_{i+1} - \\ \frac{1}{2} e_i^2 csc^4\Lambda_i - \mu_{d_i} \hat{d}_i \tilde{d}_i + d_i e_i csc^2\Lambda_i - \bar{d}_i \frac{e_i^2 csc^4\Lambda_i}{\sqrt{e_i^2 csc^4\Lambda_i + \gamma_{d_i}^2}}.\end{aligned} \tag{34}$$

Since α_i is a function of $\bar{x}_i$, x_d, $\dot{x}_d$ and estimation variables $\hat{\vartheta}_i$ and $\hat{d}_i$, it can be shown that,

$$\dot{\alpha}_i = \frac{\partial \alpha_i}{\partial \bar{x}_i} \dot{\bar{x}}_i + \frac{\partial \alpha_i}{\partial x_d} \dot{x}_d + \frac{\partial \alpha_i}{\partial \dot{x}_d} \ddot{x}_d + \frac{\partial \alpha_i}{\partial \hat{\vartheta}_1} \dot{\hat{\vartheta}}_1 + \frac{\partial \alpha_i}{\partial \hat{d}_i} \dot{\hat{d}}_i. \tag{35}$$

Considering (35), $\dot{\alpha}_i$ is a continuous function and has a maximum constant value M_i in the compact set $\Omega_{x_d} \times \Omega_i$, for given initial conditions, where $\Omega_i := \{[e_i, \tilde{\vartheta}_i, \tilde{d}_i, \chi_{i+1}]^T : (k_{e_i}^2 cot\Lambda_i)/\pi + \frac{1}{2}\tilde{\vartheta}_i^T \Gamma_i^{-1} \tilde{\vartheta}_i + \frac{1}{2}\chi_i^2 + \frac{1}{2}\tilde{d}_i^2 < \delta_i\}$ [29, 44]. So, based on Young's inequality,

$$\begin{aligned}|\dot{\alpha}_i \chi_{i+1}| &\leq \frac{\chi_{i+1}^2}{2} + \frac{M_i^2}{2}, \\ \varphi_i e_i e_{i+1} csc^2\Lambda_i &\leq \frac{\varphi_i^2 e_{i+1}^2}{2} + \frac{e_i^2 csc^4\Lambda_i}{2}, \\ e_i \varphi_i \chi_{i+1} csc^2\Lambda_i &\leq k_{\varphi_i} csc^2\Lambda_i \left(\frac{e_i^2}{2} + \frac{\chi_{i+1}^2}{2}\right).\end{aligned} \tag{36}$$

Also, it is easy to obtain,

$$\begin{aligned}-\mu_i \tilde{\vartheta}_i^T \hat{\vartheta}_i &\leq -\frac{1}{2}\mu_i \|\tilde{\vartheta}_i\|^2 + \frac{1}{2}\mu_i \|\vartheta_i\|^2, \\ -\mu_{d_i} \hat{d}_i \tilde{d}_i &\leq -\frac{1}{2}\mu_{d_i} \tilde{d}_i^2 + \frac{1}{2}\mu_{d_i} \bar{d}_i^2.\end{aligned} \tag{37}$$

Finally, according to Lemma 3,

$$d_i e_i csc^2\Lambda_i - \bar{d}_i \frac{e_i^2 csc^4\Lambda_i}{\sqrt{e_i^2 csc^4\Lambda_i+\gamma_{d_i}^2}} < \bar{d}_i\gamma_{d_i}. \tag{38}$$

According to (36)-(38) and considering Lemma 2, (34) is rewritten as,

$$\dot{V}_i \le \varphi_i N(\zeta_i)\dot{\zeta}_i + \dot{\zeta}_i - \sigma_{1,i}V_i + \sigma_{2,i} + \frac{\varphi_i^2 e_{i+1}^2}{2}, \tag{39}$$

where, $\sigma_{1,i} = \min\{K_{1,i}, K_{2,i}, \mu_i/\lambda_{max}(\Gamma_i^{-1}), \mu_{d_i}\}$, $\sigma_{2,i} = \mu_i\|\vartheta_i\|^2/2 + M_i^2/2 + \mu_{d_i}\bar{d}_i^2/2 + \bar{d}_i\gamma_{d_i}$, $K_{1,i} = \gamma_i - k_{\varphi_i}/2$ and $K_{2,i} = 1/\tau_i - k_{\varphi_i}csc^2\Lambda_i/2 - 1/2$. The selection ranges of the design parameters γ_i and τ_i are as $\gamma_i > k_{\varphi_i}/2$ and $\tau_i < 2/(k_{\varphi_i}csc^2\Lambda_i + 1)$, respectively, to guarantee that $K_{1,i}$ and $K_{2,i}$ are positive.

Step n: Define $e_n = x_n - z_n$, where z_n is virtual control. Introduce a filtering of z_n via α_{n-1} which is a stabilizing function to be designed. Let α_{n-1} pass through a first order filter with a time constant τ_n as,

$$\tau_n\dot{z}_n + z_n = \alpha_{n-1}, z_n(0) = \alpha_{n-1}(0). \tag{40}$$

Define the output error of the first-order filter as, $\chi_n = z_n - \alpha_{n-1}$ where its first-time derivative yields $\dot{z}_n = -\chi_n/\tau_n$.

Define a positive definite Lyapunov function as,

$$V_n = \frac{k_{e_n}^2}{\pi}cot\Lambda_n + \frac{1}{2}\tilde{\vartheta}_n^T\Gamma_n^{-1}\tilde{\vartheta}_n + \frac{1}{2}\tilde{d}_n^2, \tag{41}$$

where, $k_{e_n} = k_{u_n}$, if $e_n > 0$, otherwise $k_{e_n} = k_{l_n}$, $\Lambda_n = \pi(1-\xi_n^2)/2$, $\xi_n = \varpi(e_n)e_n/k_{u_n} + (1-\varpi(e_n))e_n/k_{l_n}$, with $\varpi(e_n) = 1$ if $e_n > 0$, otherwise $\varpi(e_n) = 0$, $\Gamma_n = \Gamma_n^T > 0$ is design matrix, $\tilde{\vartheta}_n = \hat{\vartheta}_n - \vartheta_n$ and $\tilde{d}_n = \hat{d}_n - \bar{d}_n$, where $\hat{\vartheta}_n$ and $\hat{d}_n$ are estimations of ϑ_n and $\bar{d}_n$, respectively. It should be noted that V_n is continuous in the set $\Omega_{e_n} = \{e_n : k_{l_n} < e_n < k_{u_n}\}$. The Lyapunov function V_n is positive definite, where the first term captures the BLF characteristics of modified tracking error ξ_n. The first-time derivative of (41), can be obtained as,

$$\dot{V}_n = \frac{2k_{e_n}\dot{k}_{e_n}}{\pi}cot\Lambda_n + k_{e_n}^2\xi_n\dot{\xi}_n csc^2\Lambda_n + \tilde{\vartheta}_n^T\Gamma_n^{-1}\dot{\hat{\vartheta}}_n + \tilde{d}_n\dot{\hat{d}}_n. \tag{42}$$

Considering the definition of ξ_n and χ_n, with dynamic response of x_n, the time derivative of ξ_n is obtained as,

$$\dot{\xi}_n = \varpi(e_n)\frac{\left(\vartheta_n^T\phi_n + \varphi_n g_s u_a + \varphi_n D + d_n + \frac{\chi_n}{\tau_n} - e_n\frac{\dot{k}_{u_n}}{k_{u_n}}\right)}{k_{u_n}} + \left(1-\varpi(e_n)\right)\frac{\left(\vartheta_n^T\phi_n + \varphi_n g_s u_a + \varphi_n D + d_n + \frac{\chi_n}{\tau_n} - e_n\frac{\dot{k}_{l_n}}{k_{l_n}}\right)}{k_{l_n}}. \tag{43}$$

Design the control input u_d as,

$$u_d = N(\zeta_n)\omega_n, \tag{44}$$

with,

$$\omega_n = \hat{\vartheta}_n^T\phi_n + \frac{\chi_n}{\tau_n} + \gamma_n e_n - e_n\frac{\dot{k}_{e_n}}{k_{e_n}} + \frac{\sin(2\Lambda_n)k_{e_n}\dot{k}_{e_n}}{\pi e_n} + \hat{d}_n\frac{e_n csc^2\Lambda_n}{\sqrt{e_n^2 csc^4\Lambda_n + \gamma_{d_n}^2}}, \tag{45}$$

and,

$$\dot{\zeta}_n = e_n\omega_n csc^2\Lambda_n, \tag{46}$$

where, γ_n and γ_{d_n} are positive design parameters. Also, construct the adaption laws $\hat{\vartheta}_n$ and $\hat{d}_n$ as,

$$\dot{\hat{\vartheta}}_n = \Gamma_n(e_n\phi_n csc^2\Lambda_n - \mu_n\hat{\vartheta}_n), \tag{47}$$

$$\dot{\hat{d}}_n = \frac{e_n^2 csc^4\Lambda_n}{\sqrt{e_n^2 csc^4\Lambda_n + \gamma_{d_n}^2}} - \mu_{d_n}\hat{d}_n, \tag{48}$$

where, μ_n and μ_{d_n} are positive design parameters.

Now using (44)-(48) and considering the actuator fault (7), $\dot{V}_n$, using (42), can be rewritten as,

$$\dot{V}_n = gN(\zeta_n)\dot{\zeta}_n + \dot{\zeta}_n - \gamma_n e_n^2 csc^2\Lambda_n + e_n\varphi_n\psi csc^2\Lambda_n - \mu_n\tilde{\vartheta}_n^T\hat{\vartheta}_n - \mu_{d_n}\hat{d}_n\tilde{d}_n + d_n e_n csc^2\Lambda_n - \tag{49}$$

$$\bar{d}_n \frac{e_n^2 csc^4 \Lambda_n}{\sqrt{e_n^2 csc^4 \Lambda_n + \gamma_{d_n}^2}}.$$

where, $g = \rho_f \varphi_n g_s$ and $\psi = g_s \phi_f + D$. It is obvious that ψ is bounded as, $|\psi| < \bar{\psi}$, where, $\bar{\psi} = \bar{g}_s \bar{\phi} + \bar{D}$ is an unknown positive constant.

Based on Young's inequality,

$$e_n \varphi_n \psi csc^2 \Lambda_n \leq \frac{e_n^2 csc^4 \Lambda_n}{2} + \frac{k_{\varphi_n}^2 \bar{\psi}^2}{2}. \tag{50}$$

Also, it is easy to obtain,

$$-\mu_n \tilde{\vartheta}_n^T \hat{\vartheta}_n \leq -\frac{1}{2}\mu_n \left\|\tilde{\vartheta}_n\right\|^2 + \frac{1}{2}\mu_n \|\vartheta_n\|^2, \tag{51}$$

$$-\mu_{d_n} \hat{d}_n \tilde{d}_n \leq -\frac{1}{2}\mu_{d_n} \tilde{d}_n^2 + \frac{1}{2}\mu_{d_n} \bar{d}_n^2. \tag{52}$$

Finally, according to Lemma 3,

$$d_n e_n csc^2 \Lambda_n - \bar{d}_n \frac{e_n^2 csc^4 \Lambda_n}{\sqrt{e_n^2 csc^4 \Lambda_n + \gamma_{d_n}^2}} < \bar{d}_n \gamma_{d_n}. \tag{53}$$

According to (50)-(53) and considering Lemma 2, (49) can be rewritten as,

$$\dot{V}_n \leq gN(\zeta_n)\dot{\zeta}_n + \dot{\zeta}_n - \sigma_{1,n} V_n + \sigma_{2,n}, \tag{54}$$

where, $\sigma_{1,n} = \min\{K_{2,n}, \mu_n/\lambda_{max}(\Gamma_n^{-1}), \mu_{d_n}\}$, $\sigma_{2,n} = \mu_n \|\vartheta_n\|^2/2 + k_{\varphi_n}^2 \bar{\psi}^2/2 + \mu_{d_n} \bar{d}_n^2/2 + \bar{d}_n \gamma_{d_n}$, and $K_{2,n} = \gamma_n - csc^2 \Lambda_n/2$. The selection range of the design parameter γ_n is then as $\gamma_n > csc^2 \Lambda_n/2$, to guarantee that $K_{2,n}$ is positive.

Remark 5: Considering the definition of ω_i in (15), (30) and (45) for $i = 1, \dots, n$, when e_i approaches to zero, employing L'Hospital's rule, the term $\sin(2\Lambda_i)\, k_{e_i} \dot{k}_{e_i}/\pi e_i$ approaches to zero, thus the singularity will not occur in (15), (30) and (45). However, since digital computers cannot evaluate 0/0, in the implementation step, the Maclaurin series with the first term is used to solve the problem. Accordingly, in (15), (30) and (45), $\sin(2\Lambda_i)\, k_{e_i} \dot{k}_{e_i}/\pi e_i$ is replaced with $\dot{k}_{e_i} e_i / k_{e_i}$, when $|e_i| < \varepsilon$, for some small positive ε.

Remark 6: It is easy to show using L'Hospital's rule, that the BLF terms in (11), (26) and (41), i.e. $k_{e_i}^2 cot \Lambda_i/\pi$ for $i = 1, \dots, n$, approaches to $e_i^2/2$, as the bounding $|k_{e_i}|$ approaches infinity. This shows that the presented BLF term can represent the mathematical equivalent of the well-known quadratic Lyapunov function (QLF). In fact, the considered BLF terms captures the QLF behaviour as the constraints are arbitrarily large enough, i.e., where there are no constraints on the tracking errors. So, the unique characteristic of the proposed controller design framework, is that when no constraint is required, one can simply replace BLF terms in (11), (26) and (41) with equivalent QLF terms. Note that the logarithm BLF like [30], or secant BLF like [26], will not have such property.

Remark 7: In this paper, with the aid of DSC, i.e., the low pass filters (10), (25) and (40), the problem of repetitive differentiation of the virtual controllers, is eliminated. This problem is obvious in several previous works, e.g., [23], in which at the step i, the partial derivative of the virtual controller α_{i-1} is needed in the controller design procedure, with respect to $\bar{x}_i$, $[x_d, \dots, x_d^{(i-1)}]$, ζ_i, $\hat{\vartheta}_i$ and $\hat{d}_i$, $i = 1, \dots, n$, which increases the implementation complexity numerically and practically (see equation (18) and (32) in [23]). It is worth noting that, when the (10), (25) and (40) are adopted, the orders of α_{i-1} and $cot\Lambda_i$ are reduced from $p \geq 2n$ to $p = 2$ and from $m \geq \max(3, n)$ to $m = 1$, respectively. More details on the efficiency of DSC on the reduction of computational complexity of the control schemes are available in [39].

Now, the main property of the designed approach is given in following theorem.

Theorem 1. Consider the class of uncertain disturbed nonlinear systems (1), with asymmetric non-smooth input saturation with unknown time varying slope (2), approximated with (4), and actuator fault (7), under Assumptions 1-5. If initial conditions satisfy $e_i(0) \in \{e_i: |e_i(0)| < k_{e_i}\}$ for $i = 1, \dots, n$, via utilizing control inputs (14), (29) and (44) with adaption laws (16)-(18), (31)-(33) and (46)-(48), then, the following objectives are achieved.

(i) All the states and signals of the closed-loop system are bounded;
(ii) The constraint sets $\Omega_{e_i} = \{e_i: k_{l_i} < e_i < k_{u_i}\}$ are never violated for $i = 1, \dots, n$ which in turn leads the output y to track $x_d(t)$ to a bounded compact set $\Omega_y := \{y(t) \in \mathbb{R}: \underline{k}_{c_1}(t) < y(t) < \bar{k}_{c_1}(t)\}$.
(iii) The tracking error e_1 can be made small by the proper choice of the design parameters.

Proof. Multiplying both sides of (54) by $e^{\sigma_{1,n}t}$ yields,

$$d(V_n(t)e^{\sigma_{1,n}t})/dt \le \left(gN(\zeta_n)\dot{\zeta}_n + \dot{\zeta}_n + \sigma_{2,n}\right)e^{\sigma_{1,n}t}. \tag{55}$$

Thus, integration of (55) over $[0, t]$, becomes,

$$V_n(t) \le \sigma_{2,n}/\sigma_{1,n} + (V_n(0) - \sigma_{2,n}/\sigma_{1,n})e^{-\sigma_{1,n}t} + e^{-\sigma_{1,n}t}\int_0^t (gN(\zeta_n) + 1)\dot{\zeta}_n e^{\sigma_{1,n}\tau} d\tau. \tag{56}$$

Furthermore, considering $\sigma_{2,n}/\sigma_{1,n} > 0$ and $\lim_{t\to\infty} e^{-\sigma_{1,n}t} = 0$, (56) becomes,

$$V_n(t) \le c_{1,n} + e^{-\sigma_{1,n}t}\int_0^t (gN(\zeta_n) + 1)\dot{\zeta}_n e^{\sigma_{1,n}\tau} d\tau. \tag{57}$$

where, $c_{1,n} = \sigma_{2,n}/\sigma_{1,n} + V_n(0)$. Also, g satisfies the conditions in Lemma 1. Accordingly, considering (57), it can be stated that V_n and ζ_n are bounded, and accordingly $(k_{e_n}^2/\pi)cot\Lambda_n$, $\tilde{\vartheta}_n$ and $\tilde{d}_n$ are bounded, which in turn leads to boundedness of e_n.

Replacing $i = n - 1$ in (39), one can obtain,

$$\dot{V}_{n-1}(t) \le \varphi_{n-1}N(\zeta_{n-1})\dot{\zeta}_{n-1} + \dot{\zeta}_{n-1} - \sigma_{1,n-1}V_{n-1} + \sigma_{2,n-1} + \frac{\varphi_{n-1}^2 e_n^2}{2}. \tag{58}$$

In similar manner, multiplying both sides of (58) by $e^{\sigma_{1,n-1}t}$ yields,

$$d(V_{n-1}(t)e^{\sigma_{1,n-1}t})/dt \le \left(\varphi_{n-1}N(\zeta_{n-1})\dot{\zeta}_{n-1} + \dot{\zeta}_{n-1} + \sigma_{2,n-1} + \frac{\varphi_{n-1}^2 e_n^2}{2}\right)e^{\sigma_{1,n-1}t}. \tag{59}$$

Thus, integration of (59) over $[0, t]$, becomes,

$$\begin{gathered} V_{n-1}(t) \le \sigma_{2,n-1}/\sigma_{1,n-1} + \left(V_{n-1}(0) - \sigma_{2,n-1}/\sigma_{1,n-1}\right)e^{-\sigma_{1,n-1}t} + e^{-\sigma_{1,n-1}t}\int_0^t \left(\varphi_{n-1}N(\zeta_{n-1})\dot{\zeta}_{n-1} + \right. \\ \left. \dot{\zeta}_{n-1}\right)e^{\sigma_{1,n-1}\tau} d\tau + e^{-\sigma_{1,n-1}t}\int_0^t \frac{\varphi_{n-1}^2 e_n^2}{2} e^{\sigma_{1,n-1}\tau} d\tau. \end{gathered} \tag{60}$$

Furthermore, considering $\sigma_{2,n-1}/\sigma_{1,n-1} > 0$ and $\lim_{t\to\infty} e^{-\sigma_{1,n-1}t} = 0$, (60) becomes,

$$\begin{gathered} V_{n-1}(t) \le \\ \sigma_{2,n-1}/\sigma_{1,n-1} + V_{n-1}(0) + e^{-\sigma_{1,n-1}t}\int_0^t (\varphi_{n-1}N(\zeta_{n-1}) + 1)\dot{\zeta}_{n-1}e^{\sigma_{1,n-1}\tau} d\tau + \\ e^{-\sigma_{1,n-1}t}\int_0^t \frac{\varphi_{n-1}^2 e_n^2}{2} e^{\sigma_{1,n-1}\tau} d\tau. \end{gathered} \tag{61}$$

Now, considering boundedness of e_n, the last term of (61), is rewritten as,

$$e^{-\sigma_{1,n-1}t}\int_0^t \frac{\varphi_{n-1}^2 e_n^2}{2} e^{\sigma_{1,n-1}\tau} d\tau \le \frac{e^{-\sigma_{1,n-1}t}\varphi_{n-1}^2}{2} \operatorname{Sup}_{\tau\in[0,t]} e_n^2(\tau)\int_0^t e^{\sigma_{1,n-1}\tau} d\tau \le m_{1,n-1}, \tag{62}$$

where, $m_{1,n-1} = \left(\varphi_{n-1}^2 \operatorname{Sup}_{\tau\in[0,t]} e_n^2(\tau)\right)/2\sigma_{1,n-1}$. Now, considering (62), (61) can be rewritten as,

$$V_{n-1}(t) \le c_{1,n-1} + e^{-\sigma_{1,n-1}t}\int_0^t (\varphi_{n-1}N(\zeta_{n-1}) + 1)\dot{\zeta}_{n-1}e^{\sigma_{1,n-1}\tau} d\tau. \tag{63}$$

where, $c_{1,n-1} = \sigma_{2,n-1}/\sigma_{1,n-1} + V_{n-1}(0) + m_{1,n-1}$.

Also, φ_{n-1} satisfies the conditions in Lemma 1. Accordingly, considering (63), it can be stated that V_{n-1} and ζ_{n-1} are bounded, and accordingly $\left(k_{e_{n-1}}^2 cot\Lambda_{n-1}\right)/\pi$, $\tilde{\vartheta}_{n-1}$ and $\tilde{d}_{n-1}$ are bounded, which in turn leads to boundedness of e_{n-1}. In the same manner, the previous procedure can be repeated for $i = n - 2, \dots, 1$. In turn, it can be proved that V_i and ζ_i, and accordingly $\left(k_{e_i}^2 cot\Lambda_i\right)/\pi$, $\tilde{\vartheta}_i$ and $\tilde{d}_i$ are bounded, which in turn leads to boundedness of e_i.

From the abovementioned analysis, the objectives (i), (ii) and (iii) are achieved as follows.

(i) Consider the boundedness of V_i, e_i, and ζ_i, for $i = 1, \dots, n$. Therefore, x_i is bounded. Now, from the boundedness of e_i, $\tilde{\vartheta}_i$ and $\tilde{d}_i$, the boundedness of $\hat{\vartheta}_i$, $\hat{d}_i$, ω_i, α_i and u_d are easily concluded.

(ii) The boundedness of $\left(k_{e_i}^2 cot\Lambda_i\right)/\pi$, $i = 1, \dots, n$, implies that e_i belongs to the set $\Omega_{e_i} = \left\{e_i: k_{l_i} < e_i < k_{u_i}\right\}$. Using the result for $i = 1$, makes e_1 belong to set $\Omega_{e_1} = \left\{e_1: k_{l_1} < e_1 < k_{u_1}\right\}$. Accordingly, x_1 stays in the set, $\Omega_{x_1} = \left\{x_1: k_{l_1} + x_d < x_1 < k_{u_1} + x_d\right\}$. On the other hand, considering Assumption 4, $k_{u_1} = \bar{k}_{c_1} - x_d$ and $k_{l_1} = \underline{k}_{c_1} - x_d$. Also, considering (1), $y = x_1$. Consequently, y stays in the set, $\Omega_y = \left\{y: \underline{k}_{c_1} < y < \bar{k}_{c_1}\right\}$.

(iii) Multiplying both sides of (24) by $e^{\sigma_{1,1}t}$ yields,

$$d\left(V_1(t)e^{\sigma_{1,1}t}\right)/dt \le \left(\varphi_1 N(\zeta_1)\dot{\zeta}_1 + \dot{\zeta}_1 + \sigma_{2,1} + \frac{\varphi_1^2 e_2^2}{2}\right)e^{\sigma_{1,1}t}. \tag{64}$$

Thus, integration of (59) over $[0, t]$, becomes,

$$V_1(t) \le \sigma_{2,1}/\sigma_{1,1} + \left(V_1(0) - \sigma_{2,1}/\sigma_{1,1}\right)e^{-\sigma_{1,1}t} + e^{-\sigma_{1,1}t}\int_0^t \left(\varphi_1 N(\zeta_1)\dot{\zeta}_1 + \dot{\zeta}_1\right)e^{\sigma_{1,1}\tau}\,d\tau + e^{-\sigma_{1,1}t}\int_0^t \frac{\varphi_1^2 e_2^2}{2} e^{\sigma_{1,1}\tau}\,d\tau. \tag{65}$$

Now, considering the boundedness of e_2, the last term of (65), can be rewritten as,

$$e^{-\sigma_{1,1}t}\int_0^t \frac{\varphi_1^2 e_2^2}{2} e^{\sigma_{1,1}\tau}\,d\tau \le \frac{e^{-\sigma_{1,1}t}\varphi_1^2}{2}\mathrm{Sup}_{\tau\in[0,t]}\, e_2^2(\tau)\int_0^t e^{\sigma_{1,1}\tau}\,d\tau \le m_{1,1}, \tag{66}$$

where, $m_{1,1} = \left(\varphi_1^2\, \mathrm{Sup}_{\tau\in[0,t]}\, e_2^2(\tau)\right)/2\sigma_{1,1}$. Also, letting $M_{1,1}$ be the upper bound of $e^{-\sigma_{1,1}t}\int_0^t (\varphi_1 N(\zeta_1) + 1)\dot{\zeta}_1 e^{\sigma_{1,1}\tau}\,d\tau$. Now, considering (65), (66) can be rewritten as,

$$V_1(t) \le \Delta_1 + \left(V_1(0) - \sigma_{2,1}/\sigma_{1,1}\right)e^{-\sigma_{1,1}t}. \tag{67}$$

where, $\Delta_1 = \sigma_{2,1}/\sigma_{1,1} + M_{1,1} + m_{1,1}$. Then, one can obtain,

$$\frac{k_{e_1}^2}{\pi} cot\Lambda_1 \le \Delta_1 + \left(V_1(0) - \sigma_{2,1}/\sigma_{1,1}\right)e^{-\sigma_{1,1}t}. \tag{68}$$

Further, inequality (68) becomes

$$|e_1| < \Theta, \tag{69}$$

where, $\Theta = k_{e_1}\sqrt{1 - 2cot^{-1}\left(\pi\left(\Delta_1 + \left(V_1(0) - \sigma_{2,1}/\sigma_{1,1}\right)e^{-\sigma_{1,1}t}\right)/k_{e_1}^2\right)/\pi}$. If $V_1(0) = \sigma_{2,1}/\sigma_{1,1}$, then it holds that $|e_1| < k_{e_1}\sqrt{1 - 2cot^{-1}\left(\pi\Delta_1/k_{e_1}^2\right)/\pi}$. If $V_1(0) \neq \sigma_{2,1}/\sigma_{1,1}$, it can be concluded that given any $\Theta > k_{e_1}\sqrt{1 - 2cot^{-1}\left(\pi\Delta_1/k_{e_1}^2\right)/\pi}$, there exists T such that for any $t > T$, it has $|e_1| < \Theta$. As, $t \to \infty$, $|e_1| < k_{e_1}\sqrt{1 - 2cot^{-1}\left(\pi\Delta_1/k_{e_1}^2\right)/\pi}$, which implies e_1 can be made arbitrarily small by selecting the design parameters appropriately.

Considering Definition 3, and objectives (i), (ii) and (iii), it is guaranteed that the closed-loop system is UUB. This completes the proof. ■

3.2. Generating state constraints.

As it is assumed in Theorem 1, the initial conditions should be set within the desired bounds. Thus, to have stable and bounded control we need to enlarge the initial values of constraints to cover the initial system states. Suppose that we need to design static constraints for the system with an initial condition, which is far from the desired trajectory. In that case, we have to choose a constant constraint, which is far from the desired trajectory and keep it to remain constant as time goes by. Accordingly, due to the probable large distance from the constraint with the real trajectory in the rest of movement, such a constraint may be useless in practice. On the other hand, suppose the situation has time-varying, but symmetric constraints. Such constraints can be helpful in the case of designing a bound for the states, which are located on the matching side with the desired trajectory. However, for the opposite side, due to symmetry, we have to choose constraints that are far from the desired trajectory. This paper introduces a systematic way to design an asymmetric time-varying constraint set that can be relaxed with any initial condition while still satisfying the design requirements. Using the presented general procedure, the constraint boundaries can cover any initial conditions, and they then exponentially tend to be close to the desired trajectories. We consider the initial condition, desired trajectory and the required constraint bounding to formulate the constraint. Considering Assumption 4, the tracking constraints are as, $\bar{k}_{c_i}(t) = k_{u_i}(t) + x_d^{(i-1)}(t)$ and $\underline{k}_{c_i}(t) = k_{l_i}(t) + x_d^{(i-1)}(t)$. Now, to relax the bounded initial condition, the tracking error bounds $k_{u_i}(t)$ and $k_{l_i}(t)$ are defined as,

$$\begin{aligned} k_{u_i}(t) &= \bar{a}_i e^{-t} + \bar{\Delta}_{u_i}(t), \\ k_{l_i}(t) &= \underline{a}_i e^{-t} + \underline{\Delta}_{l_i}(t), \end{aligned} \tag{70}$$

respectively, where $\bar{a}_i$ and $\underline{a}_i$ are presented as differences between initial conditions and their desired trajectories, and are defined as, if $x_i(0) > x_d^{(i-1)}(0)$ then $\bar{a}_i = x_i(0) - x_d^{(i-1)}(0)$ and $\underline{a}_i = 0$, else, $\bar{a}_i = 0$ and $\underline{a}_i = x_i(0) - x_d^{(i-1)}(0)$, where $x_i(0)$ is an initial value of the i^{th} state. Also, $\bar{\Delta}_{u_i}$ and $\underline{\Delta}_{l_i}$ are the preferred upper and lower bounds from the desired trajectory $x_d^{(i-1)}(t)$, respectively, to be selected by the designer. It should be noted that $\bar{\Delta}_{u_i}$ and $\underline{\Delta}_{l_i}$ can be small constants or time variables. Accordingly, the overall tracking constraint trajectories can be rewritten as,

$$\begin{aligned} \bar{k}_{c_i}(t) &= \bar{a}_i e^{-t} + x_d^{(i-1)}(t) + \bar{\Delta}_{u_i}(t), \\ \underline{k}_{c_i}(t) &= \underline{a}_i e^{-t} + x_d^{(i-1)}(t) + \underline{\Delta}_{l_i}(t). \end{aligned} \tag{71}$$

Note that upper, and lower constraints presented by (71) consist of three parts:

1) The first term, $\bar{a}_i e^{-t}$ or $\underline{a}_i e^{-t}$, boosts the initial values of the constraint close to the initial values of the desired trajectory in their matching side, since $\lim_{t\to 0} \bar{a}_i e^{-t} = \bar{a}_i$ and $\lim_{t\to 0} \underline{a}_i e^{-t} = \underline{a}_i$. Note that, as it is clear from the formation of this term, after the initial time, the constraint tends to the desired trajectory exponentially, and then as $\lim_{t\to\infty} \bar{a}_i e^{-t} = \lim_{t\to\infty} \underline{a}_i e^{-t} = 0$, this term will disappear as the time goes by. Further, note that this term then remains to be zero, for the opposite side of the initial condition with the desired trajectory.

2) The second term, $x_d^{(i-1)}(t)$, simply makes the constraint follow the trend of the desired trajectory.

3) The third term, $\bar{\Delta}_{u_i}$ and $\underline{\Delta}_{l_i}$, defines the required distance between the constraint and the desired trajectory.

Remark 8: In most of the previous works like [4, 12, 13, 23, 24, 29, 44, 45], the initial condition is assumed to be in a compact set which lies within the given constraints, to have a stabilizing controller developed. This leads to selections of constraints that are far from the desired trajectories. However, this is not a practical assumption, and accordingly, is relaxed in this paper, systematically, taking advantage of asymmetric time-varying constraints associated with the initial condition, and exponential terms $\bar{a}_i e^{-t}$ and $\underline{a}_i e^{-t}$ in (71). Also, different from previous studies on constrained control of the dynamical system, e.g., [5, 26, 30, 32], in the systematic scheme introduced in this paper on generating state constraints, the designer only needs to choose the required bound $\bar{\Delta}_{u_i}$ and $\underline{\Delta}_{l_i}$. By that means the desired constraints are automated which satisfy all required considerations of covering the initial condition, following of desired trajectory trend, and proper bounding.

Remark 9: In designing the first term of (71), we propose an exponential trend for convergence of the constraint trajectory from the initial condition to the desired trajectory using $\bar{a}_i e^{-t}$ and $\underline{a}_i e^{-t}$. However, if more speedy convergence is required e.g., in speedy practical systems, or while tracking with a small execution time, the first term of (71) can be modified by adding a convergence speed constant $\delta > 1$ as $\bar{a}_i e^{-\delta t}$, and $\underline{a}_i e^{-\delta t}$. Note that choosing $\delta < 1$ can result in slow convergence, which can be desired in some practical systems e.g. systems with slow dynamic response, e.g. wind turbines with large rotor inertia [9, 10].

3.3. Controller design algorithm.

From the previous discussions, the procedure for the controller design is given as the following algorithm.

Algorithm 1. Full State Constrained Fault Tolerant Control Design of dynamic systems with Unknown Control Gain

Inputs:

States x_i for $i = 1, \ldots, n$, and desired trajectories x_d, $\dot{x}_d$.

Initialization:

Select appropriately design parameters ε, δ, η, γ_i, γ_{d_i}, Γ_i, μ_i, μ_{d_i}, $\bar{\Delta}_{u_i}$, $\underline{\Delta}_{l_i}$, and τ_j, for $i = 1, \dots, n$ and $j = 2, \dots, n$.
Calculate $\bar{a}_i$, $\underline{a}_i$, k_{u_i}, k_{l_i}, $\dot{k}_{u_i}$, and $\dot{k}_{l_i}$, for $i = 1, \dots, n$.

Control Computation:

Solve adaptation laws to find $\hat{\vartheta}_1$ in (17), $\hat{d}_1$ in (18), $\hat{\vartheta}_i$ in (32), $\hat{d}_i$ in (33) for $i = 1, \dots, n-1$, $\hat{\vartheta}_n$ in (47) and $\hat{d}_n$ in (48).
For $i = 1, \dots, n$
If $|e_i| < \varepsilon$, then
Replace $sin(2\Lambda_i)\, k_{e_i}\dot{k}_{e_i}/\pi e_i$ by $\dot{k}_{e_i}e_i/k_{e_i}$ in (15), (30) and (45).
End.
Calculate intermediate control functions ω_1 in (15), ω_i in (30) and ω_n in (45).
Calculate virtual controls α_1 in (14) and α_i in (29) for $i = 1, \dots, n-1$.
Solve adaptation laws to find ζ_1 in (16), z_2 in (10), ζ_i in (31), z_j in (25), for $i = 1, \dots, n-1$ and $j = 2, \dots, n-1$, ζ_n in (46), and z_n in (40).
Calculate control u_d in (44).

Output:

Calculate smoothly saturated control $S(u_d)$ using (3).

4. Numerical performance evaluation and comparison.

In this section the proposed controller is evaluated via numerical simulation. In addition, the logarithm BLF control design, as one of the most utilized BLF type function, as well as the traditional QLF control design are adopted to compare the results and signify the advantages of the proposed controller.

4.1. Controllers design.

In this section, the logarithm BLF, and the traditional QLF controllers are briefly introduced and adopted with the control procedure presented in this paper. In addition, the obtained logarithm BLF based controller is compared with the developed cotangent-type BLF.

4.1.1. Logarithm BLF based controller design.

The logarithm BLF control is one of the most utilized schemes for constrained control purpose [8, 22, 29, 30, 34]. The control design using the logarithm BLF can be simply obtained via the analysis given in Section 3.1 with some modifications. To this end, only the required modifications are addressed here for the sake of brevity, as follows.

The first intuitive change is to replace cotangent BLF terms by the logarithm ones in the augmented Lyapunov function. Thus, the $cot(\bullet)$ terms in the Lyapunov functions (11), (26) and (41) are replaced with $k_{e_1}^2 log(1/(1-\xi_1^2))/2$, $k_{e_i}^2 log(1/(1-\xi_i^2))/2$, and $k_{e_n}^2 log(1/(1-\xi_n^2))/2$, respectively. Then, ω_1 in (15), ω_i in (30), and ω_n in (45) are modified accordingly as, $\omega_1 = \hat{\vartheta}_1^T\phi_1 - \dot{x}_d + \gamma_1 e_1 + e_1/2(1-\xi_1^2) - e_1\dot{k}_{e_1}/k_{e_1} + \hat{d}_1 e_1/(1-\xi_1^2)\sqrt{(e_1/(1-\xi_1^2))^2 + \gamma_{d_1}^2} + (1-\xi_1^2)\dot{k}_{e_1} log(1/(1-\xi_1^2))/\xi_1$, $\omega_i = \hat{\vartheta}_i^T\phi_i + \chi_i/\tau_i + \gamma_i e_i + e_i/2(1-\xi_i^2) - e_i\dot{k}_{e_i}/k_{e_i} + \hat{d}_i e_i/(1-\xi_i^2)\sqrt{(e_i/(1-\xi_i^2))^2 + \gamma_{d_i}^2} + (1-\xi_i^2)\dot{k}_{e_i} log(1/(1-\xi_i^2))/\xi_i$, $\omega_n = \hat{\vartheta}_n^T\phi_n + \chi_n/\tau_n + \gamma_n e_n - e_n\dot{k}_{e_n}/k_{e_n} + \hat{d}_n e_n/(1-\xi_n^2)\sqrt{(e_n/(1-\xi_n^2))^2 + \gamma_{d_n}^2} + (1-\xi_n^2)\dot{k}_{e_n} log(1/(1-\xi_n^2))/\xi_n$, respectively. Note that the last terms in these modified versions, are replaced with $2\dot{k}_{e_i}e_i/k_{e_i}$, when $|e_i| < \varepsilon$, for $i = 1, \dots, n$ and some small positive ε. In addition, the adaption laws (16)-(18), (31)-(33), and (46)-(48), are modified as, $\dot{\zeta}_1 = e_1\omega_1/(1-\xi_1^2)$, $\dot{\hat{\vartheta}}_1 = \Gamma_1(e_1\phi_1/(1-\xi_1^2) - \mu_1\hat{\vartheta}_1)$, $\dot{\hat{d}}_1 = (e_1/(1-\xi_1^2))^2/\sqrt{(e_1/(1-\xi_1^2))^2 + \gamma_{d_1}^2} - \mu_{d_1}\hat{d}_1$, $\dot{\zeta}_i = e_i\omega_1/(1-\xi_i^2)$, $\dot{\hat{\vartheta}}_i = \Gamma_i(e_i\phi_i/(1-\xi_i^2) - \mu_i\hat{\vartheta}_i)$, $\dot{\hat{d}}_i = (e_i/(1-\xi_i^2))^2/\sqrt{(e_i/(1-\xi_i^2))^2 + \gamma_{d_i}^2} - \mu_{d_i}\hat{d}_i$, $\dot{\zeta}_n = e_n\omega_n/(1-\xi_n^2)$, $\dot{\hat{\vartheta}}_n = \Gamma_n(e_n\phi_n/(1-\xi_n^2) - \mu_n\hat{\vartheta}_n)$, $\dot{\hat{d}}_n = (e_n/(1-\xi_n^2))^2/\sqrt{(e_n/(1-\xi_n^2))^2 + \gamma_{d_n}^2} - \mu_{d_n}\hat{d}_n$, respectively. Following the analysis given in Section 3.1, (24), (39) and (54) hold true with $K_{1,1} = k_{e_1}^2(\gamma_1 - k_{\varphi_1}/2)$, $K_{2,1} = 1/\tau_2 - k_{\varphi_1}/(1-\xi_1^2) - 1/2$, $K_{1,i} = k_{e_i}^2(\gamma_i - k_{\varphi_i}/2)$, $K_{2,i} = 1/\tau_i - k_{\varphi_i}/(1-\xi_i^2) -$

$1/2$, and $K_{2,n} = k_{e_n}^2(\gamma_n - csc^2\Lambda_n/2)$. Accordingly, a similar theorem as Theorem 1 can be stated for the logarithm BLF that guarantees that the closed-loop system is UUB, which is not repeated here. However, in (69), Θ is replaced with, $\Theta_{log} = k_{e_1}\sqrt{1 - exp\left(-2\left(\Delta_1 + \left(V_1(0) - \sigma_{2,1}/\sigma_{1,1}\right)exp\left(-\sigma_{1,1}t\right)\right)/k_{e_1}^2\right)}$.

The initial comparison between the cotangent BLF function, which is adopted in the proposed controller, and the logarithm one in the general case is made here, and the numerical performance comparison is studied in Section 4.4 on the dynamic system, given in Section 4.2. Comparing the behavior of $\left(k_{e_i}^2 cot\Lambda_i\right)/\pi$ and $k_{e_i}^2 log(1/(1-\xi_i^2))/2$ for $i = 1, \dots, n$, which have been used in corresponding Lyapunov functions, it can be seen that the logarithm BLF approaches to the constraints faster than the cotangent one. In this case, the designed control will increase significantly, which is not a desirable issue for most of the practical systems with bounded control effort. In contrast, the cotangent BLF keeps the error away from the constraints with a considerable distance which represents a desirable characteristic of the proposed controller.

The accurate comparison of the tracking performance of the two BLF controllers, can be outlined considering Θ and Θ_{log}. For sake of simplicity, it is assumed in both cases that $V_1(0) = \sigma_{2,1}/\sigma_{1,1}$. Hence, comparing Θ and Θ_{log}, it is obvious that for small e_1 both Θ and Θ_{log} are very close to each other. However, for bigger e_1, Θ_{log} is bigger than Θ and closer to k_{e_1} while Θ is considerably away from k_{e_1}. This can be interpreted as for small e_1 the performance of both BLF controllers is almost similar. However, for larger e_1, via adoption of the logarithm BLF control, it is only guaranteed that e_1 never violates k_{e_1}. Nevertheless, as e_1 increases, e.g., due to presence of disturbances, e_1 might get really close to k_{e_1}. In contrast, the proposed controller guarantees a remarkable bound away from the constraint. By that means, using our proposed controller, a smaller tracking error can be achieved which can help our presented cotangent BLF to be desirable in practice, when a large safe-to-operate distance from constraint is needed, e.g., the wind speed operation in high wind speed situation [10].

Finally, the comparison between control efforts of both BLF controllers can be made considering corresponding ω_i's. Obviously, in the cotangent and logarithm BLF controls, the $0.5e_i csc^2\Lambda_i$ and $0.5e_i/(1-\xi_i^2)$ terms are contributing to the bounding system states, respectively. Comparing the behaviour of these two terms, evidently it can be pointed out that for small tracking error e_i, the cotangent BLF control effort is smaller than the logarithm BLF one. On the other hand, as e_i approaches to be very close to the k_{e_i}, the cotangent BLF control effort increases more than the logarithm BLF one, to keep the e_i away from k_{e_i}. It is an advantageous feature of the cotangent BLF, which avoids excessive control effort when the tracking error is small, and instead, increases the control effort when the tracking error increases, to keep a safe-to-operate bound between the error and constraint, as stated earlier.

4.1.2. QLF controller.

The stable control design based on the QLF is the most adopted one to design the adaptive controllers. This controller is implemented in this paper to further investigate the performance of the proposed controller. This controller within the backstepping framework with DSC and adaptive laws for nonlinear disturbed systems is studied in [44] and the closed loop system is proved to be UUB. Accordingly, the analytical analysis is not repeated here. To this end, the QLF controller for the dynamic system given in Section 4.2, is designed as (44) for $n = 2$, with the modifications summarized as follows: $\dot{\hat{\vartheta}}_1 = \Gamma_1(e_1\phi_1 - \mu_1\hat{\vartheta}_1)$, $\dot{\hat{d}}_1 = e_1^2/\sqrt{e_1^2 + \gamma_{d_1}^2} - \mu_{d_1}\hat{d}_1$, $\omega_1 = \hat{\vartheta}_1^T\phi_1 - \dot{x}_d + \gamma_1 e_1 + 0.5e_1 + \hat{d}_1 e_1/\sqrt{e_1^2 + \gamma_{d_1}^2}$, $\dot{\zeta}_1 = e_1\omega_1$, $\dot{\hat{\vartheta}}_2 = \Gamma_2(e_2\phi_2 - \mu_2\hat{\vartheta}_2)$, $\dot{\hat{d}}_2 = e_2^2/\sqrt{e_2^2 + \gamma_{d_2}^2} - \mu_{d_2}\hat{d}_2$, $\omega_2 = \hat{\vartheta}_2^T\phi_2 - \chi_2/\tau_2 + \gamma_2 e_2 + \hat{d}_2 e_2/\sqrt{e_2^2 + \gamma_{d_2}^2}$, and $\dot{\zeta}_2 = e_2\omega_2$.

4.2. Dynamic system parameters.

We consider the nonlinear system (1) for $n = 2$, with constants $\nu_1 = 0.1$ and $\nu_2 = [0.2, 1]^T$, $\varphi_1 = -1$ and $\varphi_2 = 2$ and we choose $\phi_1 = x_1^2$ and $\phi_2 = [x_1x_2, x_1]^T$. Also, we consider $d_1 = 0.05\, sin(4\pi t)$ and $d_2 = 0.05\, cos(4\pi t)$. The initial condition for the state vector is chosen as $x(0) = [0.1, 0.1]^T$, and the desired trajectory is defined as $y_d = 0.5\sin(t)$. The input saturation $H(u_a)$ is constructed using $\underline{\varrho} = \bar{\varrho} = 5$, and $l = 1$, when $0 < u_a < 5$, and $l = 2$, when $-2.5 < u_a < 0$. The input saturation is illustrated in Figure 3.

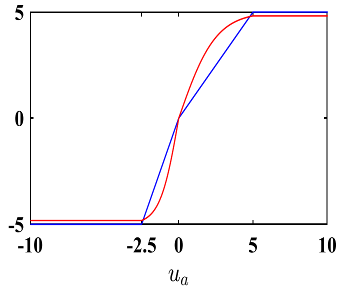

Fig. 3. The input saturation $H(u_a)$ (blue line), and its smooth estimation $S(u_a)$ (red line).

4.3. Controllers parameter values.

The proposed controller is designed as (44) associated with the virtual controller (14), and adaptive laws (17), (18), (47) and (48), considering Algorithm 1. The design parameters are selected as, $\gamma_1 = 10$, $\gamma_{d_1} = 1$, $\Gamma_1 = 1$, $\mu_1 = 1$, $\mu_{d_1} = 10$, $\tau_2 = 0.001$, $\gamma_2 = 1$, $\gamma_{d_2} = 1$, $\Gamma_2 = diag(1,1)$, $\mu_2 = [10, 10]^T$ and $\mu_{d_2} = 1$. The smooth saturation input function $S(u_a)$ is designed as (3) with $\bar{\varrho} = \underline{\varrho} = 5$, $\epsilon = 0$, and $\eta = 0.4$, as illustrated in Figure 3. In the controller design, the Nussbaum function is selected as, $N(\xi) = \xi^2\cos(\xi)$, which satisfies the Definition 1. The asymmetric tracking error constraints are selected as, $\bar{\Delta}_{u_1} = \bar{\Delta}_{u_2} = 0.03$ and $\underline{\Delta}_{l_1} = \underline{\Delta}_{l_2} = -0.03$. The required parameters of constraint trajectories (71), considering initial conditions and the desired trajectory, are obtained as $\bar{a}_1 = 0.1$, $\underline{a}_1 = 0$, $\bar{a}_2 = 0$ and $\underline{a}_2 = -0.4$. Accordingly, the upper and lower constraints for x_1 and x_2 are formed as $\bar{k}_{c_1} = 0.1e^{-t} + 0.03 + 0.5\sin(t)$, $\underline{k}_{c_1} = -0.03 + 0.5\sin(t)$, $\bar{k}_{c_2} = 0.03 + 0.5\cos(t)$ and $\underline{k}_{c_2} = -0.4e^{-t} - 0.03 + 0.5\cos(t)$, respectively. It should be noted that the same design parameter values are used in the logarithm BLF, and the traditional QLF controllers to accurately compare the results.

4.4. Numerical simulation results.

In this section the numerical simulations using the proposed cotangent BLF, logarithm BLF and QLF controllers are investigated and compared for the fault free situation. Also, in the presence of the fault, the performance of the proposed controller is evaluated. It should be noted to illustrate the points, given in Section 4.1.1, and to avoid repetitive studies, that the comparison between controllers are made only for the fault free case. Nevertheless, similar analysis can be made in the presence of faults.

4.4.1 Control evaluation in fault free case.

First, the fault free condition is considered, i.e., $\rho_f = 1$ and $\phi_f = 0$, in nonlinear dynamics given by (8) and accordingly, $u_a = u_d$. Using the proposed controller and the designed input saturation, y and y_d are illustrated in Figure 4, associated with $\bar{k}_{c_1}$ and $\underline{k}_{c_1}$. Evidently, y is tracking y_d closely, despite the presence of disturbances. Also, y never violates the given constraints. Accordingly, it can be pointed out that the constrained output tracking performance is satisfied. It should be noted in Figure 4, that since results are very close to each other and may lead to confusion, the responses of the logarithm BLF and QLF controllers are not depicted. However, to fulfil the comparison, the tracking errors of all controllers are accurately investigated afterwards.

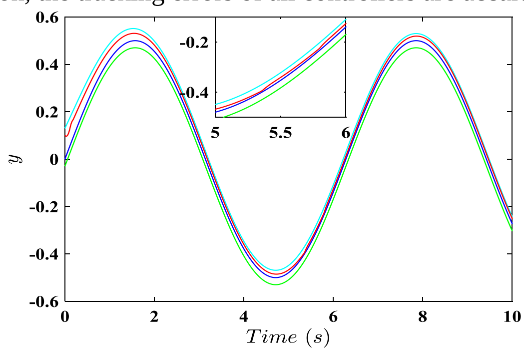

Fig. 4. y_d (dark blue line), y (red line), $\bar{k}_{c_1}$ (light blue line) and $\underline{k}_{c_1}$ (green line) in fault free case.

To accurately investigate the tracking capability of all controllers, the tracking errors e_1 and e_2 associated with k_{u_1}, k_{l_1}, k_{u_2} and k_{l_2} are illustrated in Figures 5 and 6, respectively.

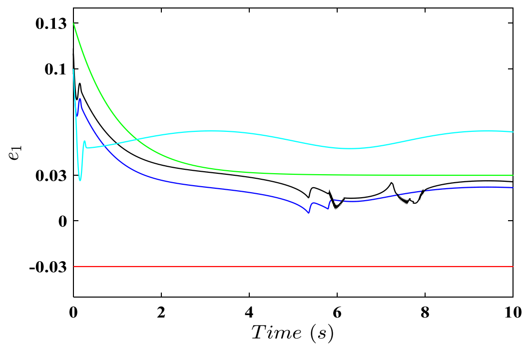

Fig. 5. Tracking error e_1 using the proposed controller (dark blue line), the logarithm BLF controller (black line), the QLF controller (light blue line), k_{u_1} (green line) and k_{l_1} (red line) in fault free case.

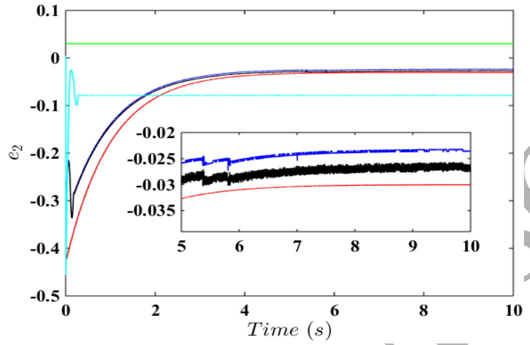

Fig. 6. Tracking error e_2 using the proposed controller (dark blue line), the logarithm BLF controller (black line), the QLF controller (light blue line), k_{u_2} (green line) and k_{l_2} (red line) in fault free case.

Figures 5 and 6, respectively, show that, using the proposed and the logarithm BLF controllers, y and x_2 track the corresponding desired trajectories, satisfactorily, while the tracking errors stay within the constraints and disturbances are attenuated. In contrast, it is obvious that the use of the QLF controller has led to small tracking errors, but it is not able to keep the tracking errors within corresponding constraints. As mentioned in Section 4.1.1, using the logarithm BLF controller, the tracking errors are kept closer to the constraints, which might lead to larger control effort. While, the proposed controller increases the distance of the tracking errors from constraints. This issue is obvious considering Figures 5 and 6 and comparing the performances of the proposed and logarithm BLF controllers.

In Figures 7, 8 and 9, the estimated $\hat{v}_1$ and $\hat{v}_2 = [\hat{v}_{2,1}, \hat{v}_{2,2}]^T$, using adaptive laws, are shown, respectively. It is obvious that all $\hat{v}_1$, $\hat{v}_{2,1}$ and $\hat{v}_{2,2}$ approach to the corresponding actual values.

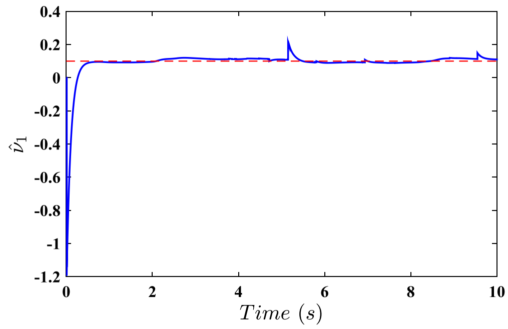

Fig. 7. The estimation (blue line) and actual value of $\hat{v}_1$ (red line).

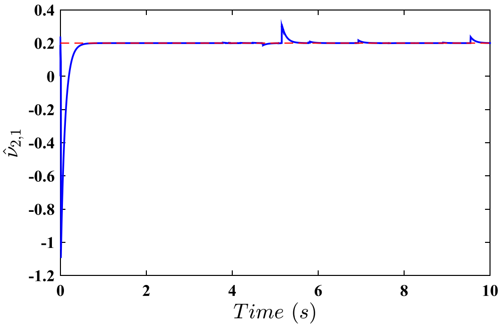

Fig. 8. The estimation (blue line) and actual value of $\hat{v}_{2,1}$ (red line).

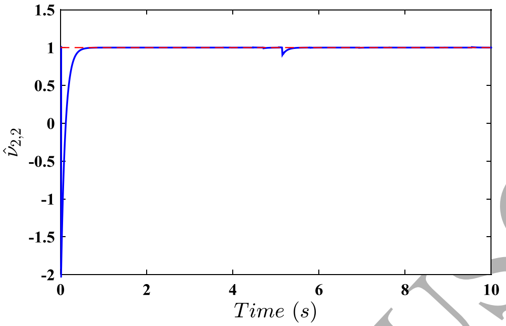

Fig. 9. The estimation (blue line) and actual value of $\hat{v}_{2,2}$ (red line).

Now, our proposed control with the smooth input saturation is evaluated. In Figure 10, smooth saturation function $S(u_d)$ using the proposed controller, the saturation function $H(u_d)$, the unsaturated control input u_d, and the logarithm BLF control effort are illustrated. Obviously, the designed cotangent-type BLF control is bounded and smooth. Also, despite the function $H(u_d)$ having sharp saturation behaviour, by using $S(u_d)$ the input is smoothly saturated and passed from each saturation period. It is worth noting that the unsaturated control input u_d violates the given bounds. On the other hand, in accordance with the Figures 5 and 6, and the analysis given in Section 4.1.1, it is obvious that the control effort of the logarithm BLF controller is considerably larger than the proposed controller one, in the time periods in which the tracking errors of the logarithm BLF controller are closer to the constraints. It should be noted that, as the QLF controller is not able to keep the tracking errors within the constraints, the corresponding control effort is not shown here.

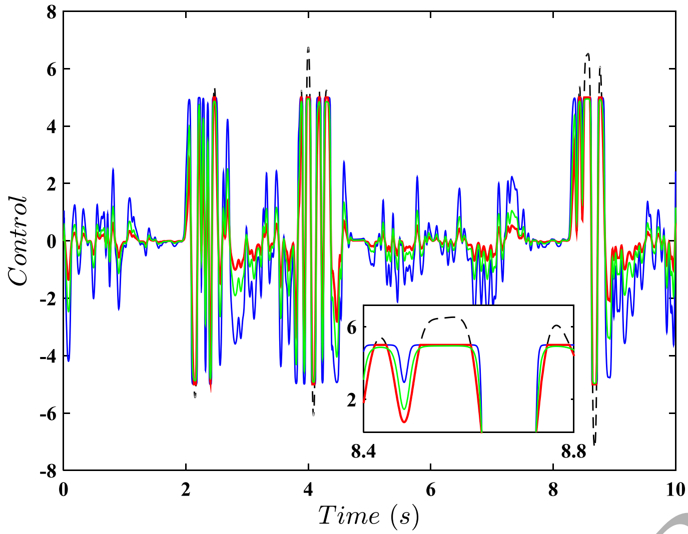

Fig. 10. Smooth input saturation $S(u_d)$ using the proposed controller (green line), input saturation $H(u_d)$ (red line), the logarithm BLF control effort (blue line), and unsaturated control input u_d (dashed black line) in fault free case.

4.4.2 Control evaluation with actuation fault.

Now, the fault tolerant capability of the designed controller is investigated. Considering the nonlinear system (8), the effectiveness loss and additive fault are selected as $\rho_f = 0.6 + 0.4\cos(\pi t/4)$ and $\phi_f = 0.2\cos(\pi t)$, respectively. Thus, $u_a = \rho_f u_d + \phi_f$. It should be noted that as the comparison between all controllers were made in previous section, and to focus on the fault tolerance capability, the proposed controller performance is only studied here.

The tracking errors e_1 and e_2 associated with corresponding constraints are illustrated in Figures 11 and 12, respectively. It is obvious that the tracking errors are bounded by constraints, the same as the fault free case. So, it can be pointed out that the proposed controller is able to satisfy the constrained tracking performance in the presence of the disturbance and fault. Also, the input u_d is smoothly saturated and passed from each saturation period, as shown in Figure 13.

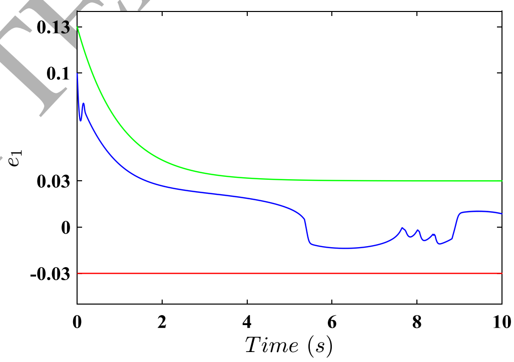

Fig. 11. Tracking error e_1 (blue line), k_{u_1} (green line) and k_{l_1} (red line) using the proposed controller in actuator fault case.

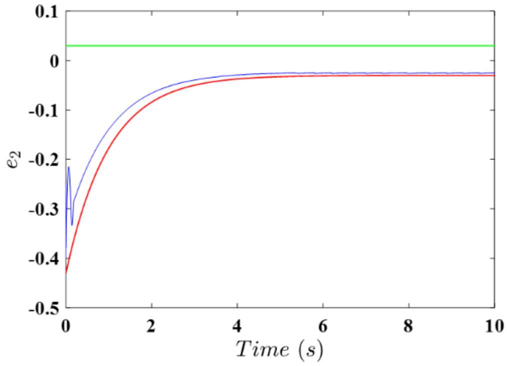

Fig. 12. Tracking error e_2 (blue line), k_{u_2} (green line) and k_{l_2} (red line) using the proposed controller in actuator fault case.

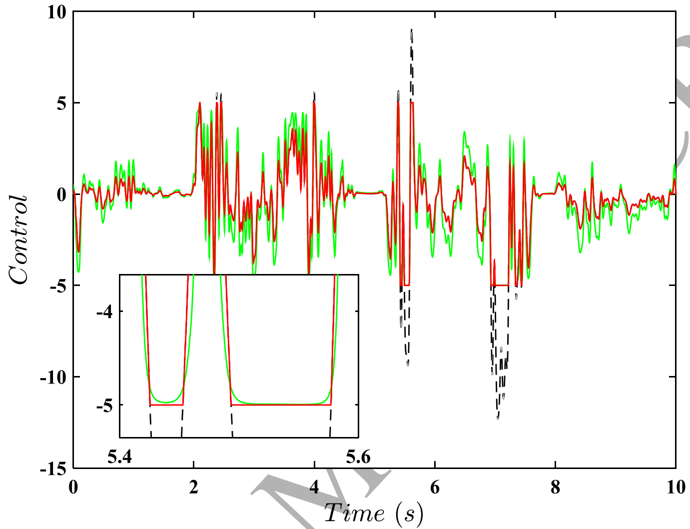

Fig. 13. Smooth input saturation $S(u_d)$ using the proposed controller (green line), input saturation $H(u_d)$ (red line), and unsaturated control input u_d (dashed black line) in the actuator fault case.

5. Conclusions.

In this paper, a backstepping design scheme based on BLF in conjunction with Nussbaum-type function, and DSC was developed for the constrained control design of nonlinear strict feedback uncertain dynamic systems subject to input saturation, actuation failure, and unknown control direction. A Nussbaum-type function was utilized to solve the problem of unknown control directions, and the complexity of repetitive derivations in the backstepping procedure was reduced employing DSC. A new cotangent-type BLF was introduced to tackle the state constraints effectively. Smooth input saturation was expressed, and the actuation faults were handled without the need for fault detection and controller reconfiguration. Compared with currently available methods, the proposed constrained control scheme has advantages, such as 1) directly exploiting the constraints on the control design, and thus avoiding error transformation, or transforming the original constrained system into an equivalent unconstrained one, 2) handling both asymmetric and time-varying constrained systems, 3) ability to provide a singularity-free control system, 4) ability to simply replace the constraints with the QLF when no constraints are required, and 5) requiring fewer parameters in the design procedure, as a result of introducing a useful Lemma. However, the salient feature of the proposed constrained controller lies in proposing a new constraint generating system, where a designer only needs to decide on a required bound to automate a constraint that can relax any initial condition and converge to the desired trajectory. It was proven that no state constraints would be violated and all the signals in the closed-loop system were bounded, in both fault free and faulty situations. Theoretical developments were verified through numerical simulation, in which the performance of the proposed controller was compared to the corresponding logarithm BLF and QLF controllers.

Reference

[1] L. An, G.-H. Yang, Improved adaptive resilient control against sensor and actuator attacks, Information Sciences, 423 (2018) 145-156.
[2] H. Badihi, Y. Zhang, H. Hong, Fault-tolerant cooperative control in an offshore wind farm using model-free and model-based fault detection and diagnosis approaches, Appl Energy, 201 (2017) 284-307.
[3] C.C. Cheah, S.P. Hou, Y. Zhao, J.-J.E. Slotine, Adaptive vision and force tracking control for robots with constraint uncertainty, IEEE/ASME Transactions on Mechatronics, 15 (2010) 389-399.
[4] Z. Chen, Z. Li, C.L.P. Chen, Adaptive Neural Control of Uncertain MIMO Nonlinear Systems With State and Input Constraints, IEEE Transactions on Neural Networks and Learning Systems, 28 (2017) 1318-1330.
[5] M. Davanipour, A.R. Khayatian, M. Dehghani, M.M. Arefi, A solution for enhancement of transient performance in nonlinear adaptive control: Optimal adaptive reset based on barrier Lyapunov function, ISAT, 80 (2018) 169-175.
[6] L. Edalati, A.K. Sedigh, M.A. Shooredeli, A. Moarefianpour, Adaptive fuzzy dynamic surface control of nonlinear systems with input saturation and time-varying output constraints, MSSP, 100 (2018) 311-329.
[7] S. Gao, B. Ning, H. Dong, Fuzzy dynamic surface control for uncertain nonlinear systems under input saturation via truncated adaptation approach, Fuzzy Sets and Systems, 290 (2016) 100-117.
[8] H. Habibi, H.R. Nohooji, I. Howard, Constrained control of wind turbines for power regulation in full load operation, in: 11th Asian Control Conference (ASCC), Australia, 2017, pp. 2813-2818.
[9] H. Habibi, H.R. Nohooji, I. Howard, Optimum efficiency control of a wind turbine with unknown desired trajectory and actuator faults, J Renew Sustain Energy, 9 (2017) 063305.
[10] H. Habibi, H.R. Nohooji, I. Howard, Adaptive PID Control of Wind Turbines for Power Regulation With Unknown Control Direction and Actuator Faults, IEEE Access, 6 (2018) 37464-37479.
[11] W. He, S. Zhang, S.S. Ge, Adaptive control of a flexible crane system with the boundary output constraint, IEEE Transactions on Industrial Electronics, 61 (2014) 4126-4133.
[12] W. He, Y. Chen, Z. Yin, Adaptive neural network control of an uncertain robot with full-state constraints, IEEE Transactions on Cybernetics, 46 (2016) 620-629.
[13] Z.J. Jia, Y.D. Song, Barrier Function-Based Neural Adaptive Control With Locally Weighted Learning and Finite Neuron Self-Growing Strategy, IEEE Transactions on Neural Networks and Learning Systems, 28 (2017) 1439-1451.
[14] X. Jin, Adaptive fault tolerant control for a class of input and state constrained MIMO nonlinear systems, International Journal of Robust and Nonlinear Control, 26 (2016) 286-302.
[15] X. Jin, Adaptive fault tolerant tracking control for a class of stochastic nonlinear systems with output constraint and actuator faults, Systems & Control Letters, 107 (2017) 100-109.
[16] X. Jin, Adaptive decentralized finite-time output tracking control for MIMO interconnected nonlinear systems with output constraints and actuator faults, International Journal of Robust and Nonlinear Control, 28 (2018) 1808-1829.
[17] Y. Li, S.S. Ge, C. Yang, Learning impedance control for physical robot–environment interaction, International Journal of Control, 85 (2012) 182-193.
[18] Y. Li, Z. Ma, S. Tong, Adaptive Fuzzy Fault-Tolerant Control of Nontriangular Structure Nonlinear Systems With Error Constraint, IEEE Transactions on Fuzzy Systems, 26 (2018) 2062-2074.
[19] Z. Li, J. Li, Y. Kang, Adaptive robust coordinated control of multiple mobile manipulators interacting with rigid environments, Automatica, 46 (2010) 2028-2034.
[20] Z. Li, S.S. Ge, M. Adams, W.S. Wijesoma, Robust adaptive control of uncertain force/motion constrained nonholonomic mobile manipulators, Automatica, 44 (2008) 776-784.
[21] H. Liu, M. Zhong, Y. Liu, A New Residual Evaluation Function Based Fault Diagnosis for a Kind of Nonlinear Systems, Asian Journal of Control, 21 (2019) 1-13.
[22] Y.-J. Liu, S. Tong, Barrier Lyapunov Functions-based adaptive control for a class of nonlinear pure-feedback systems with full state constraints, Autom, 64 (2016) 70-75.
[23] Y.-J. Liu, S. Tong, Barrier Lyapunov functions for Nussbaum gain adaptive control of full state constrained nonlinear systems, Autom, 76 (2017) 143-152.
[24] Y. Liu, J. Yu, H. Yu, C. Lin, L. Zhao, Barrier Lyapunov Functions-Based Adaptive Neural Control for Permanent Magnet Synchronous Motors With Full-State Constraints, IEEE Access, 5 (2017) 10382-10389.
[25] S. Luo, J. Wang, S. Wu, K. Xiao, Chaos RBF dynamics surface control of brushless DC motor with time delay based on tangent barrier Lyapunov function, Nonlinear Dynamics, 78 (2014) 1193-1204.
[26] H.R. Nohooji, I. Howard, L. Cui, Neural network adaptive control design for robot manipulators under velocity constraints, Journal of the Franklin Institute, 355 (2018) 693-713.
[27] R.D. Nussbaum, Some remarks on a conjecture in parameter adaptive control, Systems & Control Letters, 3 (1983) 243-246.

[28] C. Peng, E. Tian, J. Zhang, D. Du, Decentralized event-triggering communication scheme for large-scale systems under network environments, Information Sciences, 380 (2017) 132-144.
[29] Y. Qiu, X. Liang, Z. Dai, Backstepping dynamic surface control for an anti-skid braking system, Control Eng. Pract., 42 (2015) 140-152.
[30] F. Qu, S. Tong, Y. Li, Observer-based adaptive fuzzy output constrained control for uncertain nonlinear multi-agent systems, Information Sciences, 467 (2018) 446-463.
[31] H.N. Rahimi, I. Howard, L. Cui, Neural adaptive assist-as-needed control for rehabilitation robots, in: Australasian Conference on Robotics and Automation (ACRA2016), 2016.
[32] H.N. Rahimi, I. Howard, L. Cui, Neural impedance adaption for assistive human–robot interaction, Neurocomputing, 290 (2018) 50-59.
[33] H.N. Rahimi, I. Howard, L. Cui, Neural adaptive tracking control for an uncertain robot manipulator with time-varying joint space constraints, Mechanical Systems and Signal Processing, 112 (2018) 44-60.
[34] B. Ren, S.S. Ge, K.P. Tee, T.H. Lee, Adaptive neural control for output feedback nonlinear systems using a barrier Lyapunov function, ITNN, 21 (2010) 1339-1345.
[35] H. Shao, Z. Gao, X. Liu, K. Busawon, Parameter-varying modelling and fault reconstruction for wind turbine systems, Renewable Energy, 116 (2018) 145-152.
[36] Y. Song, X. Huang, C. Wen, Robust Adaptive Fault-Tolerant PID Control of MIMO Nonlinear Systems With Unknown Control Direction, IEEE Trans. Ind. Electron., 64 (2017) 4876-4884.
[37] Z.-L. Tang, S.S. Ge, K.P. Tee, W. He, Adaptive neural control for an uncertain robotic manipulator with joint space constraints, International Journal of Control, 89 (2016) 1428-1446.
[38] K.P. Tee, S.S. Ge, Control of nonlinear systems with partial state constraints using a barrier Lyapunov function, IJC, 84 (2011) 2008-2023.
[39] K.P. Tee, S.S. Ge, E.H. Tay, Barrier Lyapunov functions for the control of output-constrained nonlinear systems, Autom, 45 (2009) 918-927.
[40] K.P. Tee, R. Yan, H. Li, Adaptive admittance control of a robot manipulator under task space constraint, in: IEEE International Conference on Robotics and Automation (ICRA), 2010, pp. 5181-5186.
[41] H. Yang, Z. Liu, Active control of an elastic beam based on state and input constraints, IEEE Access, 6 (2018) 10635-10643.
[42] D.-H. Zhai, Y. Xia, Adaptive control for teleoperation system with varying time-delays and input saturation constraints, IEEE Transactions on Industrial Electronics 63 (2016) 6921 - 6929.
[43] S. Zhang, Z. Tang, S.S. Ge, W. He, Adaptive neural dynamic surface control of output constrained non-linear systems with unknown control direction, IET Control Theory & Applications, 11 (2017) 2994-3003.
[44] K. Zhao, Y. Song, C. Wen, Computationally inexpensive fault tolerant control of uncertain non-linear systems with non-smooth asymmetric input saturation and undetectable actuation failures, IET Control Theory Appl., 10 (2016) 1866-1873.
[45] K. Zhao, Y. Song, Z. Shen, Neuroadaptive Fault-Tolerant Control of Nonlinear Systems Under Output Constraints and Actuation Faults, IEEE Transactions on Neural Networks and Learning Systems, 29 (2018) 286-298.